Dalton
www.rsc.org/dalton

Ligand substitutions in Ru–Pt clusters: isolation of compounds with unusual geometries

Sophie Hermans,[a] Tetyana Khimyak,[a] Neil Feeder,[a] Simon J. Teat[b] and Brian F. G. Johnson*[a]

[a] *University Chemical Laboratories, University of Cambridge, Lensfield Road, Cambridge, UK CB2 1EW. E-mail: bfgj1@cam.ac.uk*

[b] *CLRC Daresbury Laboratory, Warrington, UK WA4 4AD*

Received 30th September 2002, Accepted 25th November 2002
First published as an Advance Article on the web 13th January 2003

Ligand substitution reactions of the COD (1,5-cyclooctadiene) ligand for CO or phosphines in the clusters $[Ru_5C(CO)_{14}Pt(COD)]$ (**1**) and $[Ru_6C(CO)_{16}Pt(COD)]$ (**2**) were investigated. Reactions with carbon monoxide gave selectively $[Ru_5CPt(CO)_{16}]$ (**3**) from **1**, but led to loss of either a ruthenium or the Pt(COD) unit from the Ru_6Pt cluster (**2**). Substitution of the COD ligand by PPh_3 in **1** gave $[Ru_5C(CO)_{14}Pt(PPh_3)_2]$ (**8**) selectively, while with dppm the main product of the reaction was $[Ru_5C(CO)_{14}Pt(\mu\text{-dppm})]$ (**10**). On the other hand, the reactions involving $[Ru_6C(CO)_{16}Pt(COD)]$ (**2**) and phosphines led mainly to extrusion of the Pt(COD) fragment and formation of Ru-only derivatives. More precisely, with triphenylphosphine, the two clusters $[Ru_6C(CO)_{16}PPh_3]$ (**16**) and $[Ru_6C(CO)_{15}(PPh_3)_2]$ (**18**) were obtained from **2**, while with dppm, the compounds $[Ru_6C(CO)_{15}(dppm)]$ (**15**) and $[Ru_6C(CO)_{13}(dppm)_2]$ (**19**) were formed. In the latter case, two additional products of increased nuclearity were isolated: $[Ru_6C(CO)_{15}Pt_2(dppm)]$ (**20**) and $[Ru_6C(CO)_{16}Pt_3(dppm)_2]$ (**21**). All the compounds described were characterised by spectroscopic methods and the structures of the new species were determined by X-ray crystallography.

Introduction

Mixed-metal Ru–Pt clusters of high nuclearity have proven to be suitable precursors for bimetallic nanoparticles that have been used as highly active hydrogenation catalysts.[1] However, few Ru–Pt clusters displaying more than five metal atoms in their cores are known;[2] hence the need to develop reliable and efficient methods for the synthesis of such compounds. We have reported recently a new method, based on chloride abstraction by silica from $[PtL_2Cl_2]$ complexes, followed by reaction with anionic ruthenium clusters, to produce Ru–Pt clusters with a chosen nuclearity in high yield.[3] In this paper, we wish to report on the use of two of these Ru–Pt clusters, *i.e.* $[Ru_5C(CO)_{14}Pt(COD)]$ **1** and $[Ru_6C(CO)_{16}Pt(COD)]$ **2**, [3] (COD = 1,5-cyclooctadiene) in reactions of ligand substitution with carbon monoxide and phosphines. These reactions led to the isolation of new compounds, in some cases with increased nuclearity, which could in turn be used as nanoparticle precursors.

Results and discussion

1. Reactions with carbon monoxide

The reaction of $[Ru_5C(CO)_{14}Pt(COD)]$ **1** with carbon monoxide has been investigated previously,[4] and gave the compound $[Ru_5CPt(CO)_{16}]$ **3** cleanly in 97% yield (Fig. 1).[4] This compound is the simple product of substitution of the COD ligand for two CO groups, and was characterised by crystallographic analysis.[4]

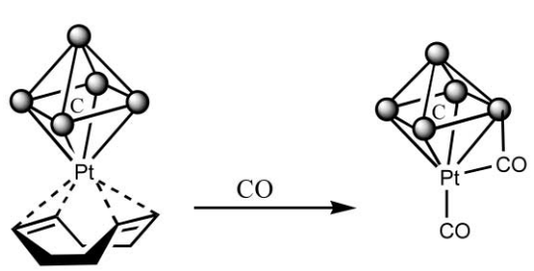

Fig. 1 Formation of $[Ru_5CPt(CO)_{16}]$ **3** from $[Ru_5C(CO)_{14}Pt(COD)]$ **1**. Shaded circles represent Ru. The carbonyl ligands attached to the ruthenium atoms are omitted for clarity.

The reactivity of $[Ru_6C(CO)_{16}Pt(COD)]$ **2** with carbon monoxide was thus also investigated. When CO gas was bubbled through a solution of $[Ru_6C(CO)_{16}Pt(COD)]$ **2** for 24 hours, three compounds could be isolated from the reaction mixture. They were identified as the known $[Ru_3(CO)_{12}]$ **4**, $[Ru_5CPt(CO)_{16}]$ **3** and $[Ru_6C(CO)_{17}]$ **5**, by comparison of their IR and mass spectra with data from the literature.[4–6] The formation of $[Ru_3(CO)_{12}]$ **4** must involve a degradation process, while $[Ru_6C(CO)_{17}]$ **5** was formed by replacement of the Pt(COD) unit by one CO ligand. The extrusion of a Pt(COD) fragment by reacting a Pt–M mixed-metal cluster with CO is not unprecedented: the reaction of $[Os_6Pt(CO)_{17}(NCMe)(COD)]$ with carbon monoxide was reported to lead to $[Os_6(CO)_{19}(NCMe)]$.[7] The formation of $[Ru_5CPt(CO)_{16}]$ **3** is more surprising. However, it might be understood by analogy with the formation of $[Ru_5C(CO)_{15}]$ **6** by loss of a $Ru(CO)_2$ unit from $[Ru_6C(CO)_{17}]$ **5** in the presence of carbon monoxide.[8] Two different isomers with different metal core geometries may be suggested for $[Ru_5CPt(CO)_{16}]$ **3** (Fig. 2): an octahedron (isomer A)

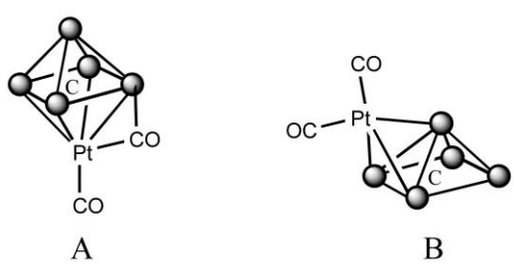

Fig. 2 Possible isomers for $[Ru_5CPt(CO)_{16}]$ **3**. Shaded circles represent Ru. The carbonyl ligands attached to ruthenium atoms are omitted for clarity.

or a mono-capped square pyramid (isomer B). According to the PSEPT rules, both geometries would be consistent with the 86 electron count for cluster **3**. Single crystals of $[Ru_5CPt(CO)_{16}]$ **3** were grown and the unit cell parameters measured, which indicated that isomer A had been obtained, as in the case of the product of reaction of $[Ru_5C(CO)_{14}Pt(COD)]$ **1** with CO.[4] The formation of isomer A from compound **2** implies that a

DOI: 10.1039/b209592k

rearrangement occurred after substitution of the COD ligand by carbonyls and loss of a $Ru(CO)_2$ unit, allowing the platinum fragment to migrate from capping a Ru_3 triangular face to capping the Ru_4C square face. By a strict equivalence with $[Ru_5C(CO)_{14}Pt(COD)]$ **1**, the main product expected from the reaction of $[Ru_6C(CO)_{16}Pt(COD)]$ **2** with carbon monoxide was $[Ru_6CPt(CO)_{18}]$ **7**. This compound would have probably displayed a mono-capped octahedral metal core, as shown in Fig. 3. This cluster could not be detected in the reaction

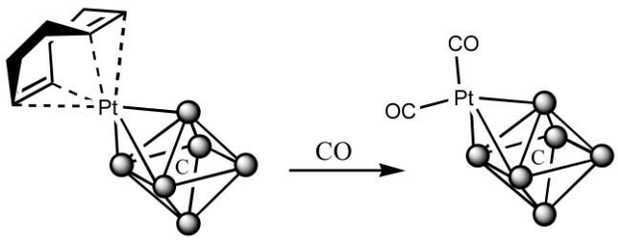

Fig. 3 Formation of $[Ru_6CPt(CO)_{18}]$ **7** from $[Ru_6C(CO)_{16}Pt(COD)]$ **2**. Shaded circles represent Ru. The carbonyl ligands attached to ruthenium atoms are omitted for clarity.

mixture, even at very short reaction times. Careful monitoring of the reaction by infrared spectroscopy and spot TLC showed that compounds **4**, **3** and **5** are formed simultaneously.

2. Attempts to substitute the COD ligand by phosphines

Cyclooctadiene is a good leaving group, and should easily be displaced by an incoming phosphine ligand. As an illustration, substitution of the COD ligand for dppe or $P(OMe)_3$ in $[Os_6Pt(CO)_{17}(NCMe)(COD)]$ was achieved and shown to result in clusters having an unchanged metallic framework.[7] The reactions of $[Ru_5C(CO)_{14}Pt(COD)]$ **1** and $[Ru_6C(CO)_{16}Pt(COD)]$ **2** with PPh_3 and dppm (= bis(diphenylphosphino)methane) were examined. It was hoped that the clusters produced would be of the type $[Ru_nC(CO)_mPtL_2]$, where $n = 5, 6$; $m = 14, 16$; and $L_2 = (PPh_3)_2$ or dppm. If these substitution reactions proved to be selective, it would open up the possibility of anchoring the clusters onto a functionalised surface, *via* pending phosphine groups, such as illustrated in Fig. 4 for $[Ru_5C(CO)_{14}Pt(COD)]$ **1**.

2.1. Attempts to substitute the COD ligand in $[Ru_5C(CO)_{14}Pt(COD)]$ 1. The cluster $[Ru_5C(CO)_{14}Pt(COD)]$ **1** was reacted with one molar equivalent of triphenylphosphine in dichloromethane. After 7 hours stirring at room temperature, a single product was isolated in 43.6% yield by thin-layer chromatography. It was identified as the desired $[Ru_5C(CO)_{14}Pt(PPh_3)_2]$ **8** on the basis of elemental analysis and spectroscopic characterisation. This compound had already been synthesised independently by reacting $[Ru_5C(CO)_{14}]^{2-}$ with $[Pt(PPh_3)_2Cl_2]$ in the presence of silica.[3] The IR, mass spectrometry and NMR results reported previously [3] were identical with those obtained here for compound **8**. The crystal structure of this compound was determined previously,[3] and shown to consist of a Ru_5Pt octahedron with a Pt-bound PPh_3 and a Ru-bound PPh_3, as

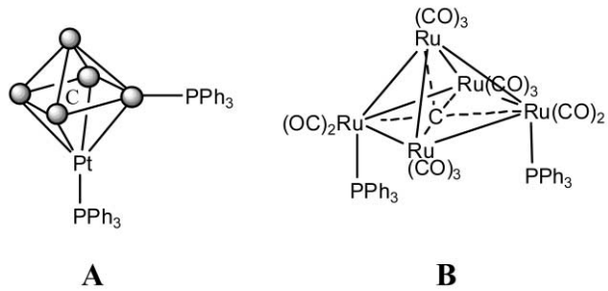

A B

Fig. 5 Structures of (A) $[Ru_5C(CO)_{14}Pt(PPh_3)_2]$ **8** (carbonyls are omitted for clarity) and (B) $[Ru_5C(CO)_{13}(PPh_3)_2]$ **9**, as determined by X-ray crystallography.[2,3]

determined by NMR (Fig. 5). The *closo*-octahedral geometry for the cluster core of **8** (86 electron count) would have also been predicted by the PSEPT rules. Here, the formation of compound **8** from $[Ru_5C(CO)_{14}Pt(COD)]$ **1** must have involved an intermediate where both phosphines were bound to the Pt atom, followed by migration of one PPh_3 to one of the adjacent Ru atoms. This kind of ligand exchange between the two metals in Ru–Pt mixed-metal clusters occurs frequently during their syntheses.[9]

When the same reaction was performed with an excess PPh_3, the platinum was expelled from the cluster, and the known $[Ru_5C(CO)_{13}(PPh_3)_2]$ **9** was formed as the main product. A secondary brown product was also isolated in very low yield from the reaction mixture. The IR spectrum for $[Ru_5C(CO)_{13}(PPh_3)_2]$ **9** fitted with data from the literature [10] and the mass spectrometry and NMR results were consistent with that formulation. Crystals of **9** suitable for X-ray diffraction analysis were obtained and the unit cell parameters fitted with the crystallographic data reported previously for that compound. Indeed, the crystal structure of $[Ru_5C(CO)_{13}(PPh_3)_2]$ **9** had already been determined,[10] and shown to consist of a Ru_5 square pyramid with two triphenylphosphine ligands terminally bound to two basal Ru atoms (Fig. 5). This geometry is in line with the 74 electron count for compound **9**. The mechanism by which this compound was formed here from $[Ru_5C(CO)_{14}Pt(COD)]$ **1** must involve first the substitution of the Pt(COD) fragment by one PPh_3, and subsequently substitution of a CO for a second PPh_3. The secondary brown compound could not be indisputably identified on the basis of the experimental evidence gathered. Its IR spectrum, with bands in the region of terminal as well as bridging CO ligands, did not bear any resemblance to that of $[Ru_5C(CO)_{14}(PPh_3)]$,[10] $[Ru_5C(CO)_{13}(PPh_3)_2]$ **9**,[10] or $[Ru_5C(CO)_{14}Pt(PPh_3)_2]$ **8** (*vide supra*). A fragment only could be obtained by mass spectrometry, at *m*/*z* 1087, corresponding to the formulation $[Ru_5C(CO)_{11}(PPh_3)]$, together with peaks of CO ligand losses and one Ph unit loss. Signals for the phenyl protons could be observed at 7.55–7.23 ppm. Two signals were obtained by ^{31}P-NMR at 43.39 and 29.43 ppm, without Pt satellites. The brown compound is thus most probably an isomer of either compound **9** or compound **8**.

$[Ru_5C(CO)_{14}Pt(COD)]$ **1** was then reacted with bis(diphenylphosphino)methane (dppm). It was hoped that substituting a

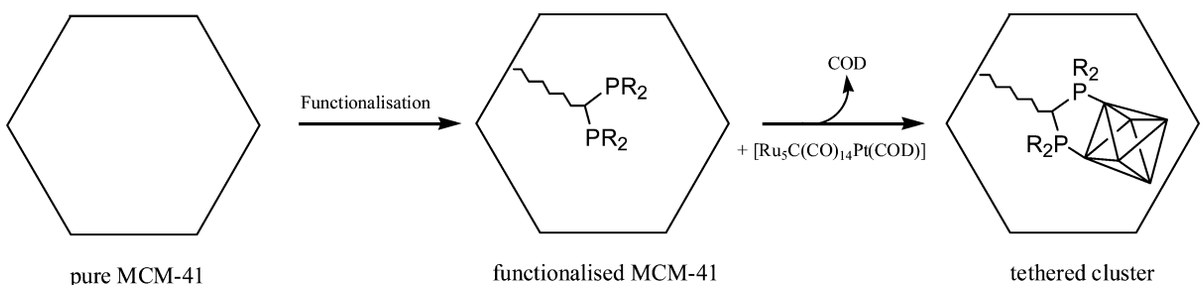

Fig. 4 Possible strategy to tether cluster compounds inside the mesopores of MCM-41, by ligand substitution for an organic tether bearing a bidentate phosphine group.

bidentate COD ligand for a bidentate diphosphine ligand would be highly selective. However, three products were isolated from the reaction mixture by thin-layer chromatography. These were identified as $[Ru_5CPt(CO)_{16}]$ **3**, $[Ru_5C(CO)_{14}Pt(\mu\text{-dppm})]$ **10** and $[Ru_5C(CO)_{11}Pt(CO)(dppm)_2]$ **11**, on the basis of analytical evidence. Compound **3** was obtained in less than 1% yield. Its IR spectrum was identical to that reported previously for that compound,[4] and the molecular peak was obtained by mass spectrometry at *m*/*z* 1162, followed by 16 CO loss peaks. The main product of the reaction was $[Ru_5C(CO)_{14}Pt(\mu\text{-dppm})]$ **10**, which was obtained in 64.3% yield. It was formulated on the basis of satisfactory elemental analysis and mass spectra. Carbonyls in bridging and terminal bonding modes were identified from the positions of the CO stretching frequencies observed by infrared spectroscopy. An IR spectrum was also recorded in cyclohexane, in order to compare with data reported in the literature for $[Ru_5C(CO)_{13}(dppm)]$ **12**, and discard that possibility.[11] The molecular peak was observed at *m*/*z* 1494 (with subsequent loss of CO ligands and Ph units), when using the electron impact ionisation technique run in positive ion mode. A mass spectrum was also obtained by electrospray ionisation technique, run in negative ion mode, in the presence of methoxide.[12,13] A peak at *m*/*z* 1520, corresponding to $[Ru_5C(CO)_{14}Pt(dppm)] + CH_3O$ (calc. 1520, $[M + MeO]^-$) was observed. The phenyl rings of dppm appeared as multiplets in the range 7.21–7.49 ppm (integral: 20H) in the ^{1}H-NMR spectrum, and 137.95–128.24 ppm in the ^{13}C-NMR spectrum. The protons of the PCH_2P group are non-equivalent and gave rise to two quartets at 5.27 ppm (integral: 1H) and at 4.77 ppm (integral: 1H) in the ^{1}H-NMR. The carbon of the PCH_2P grouping was found at 63.85 ppm by ^{13}C-NMR. The carbonyl ligands gave rise to a broad signal at 199.41 ppm in the ^{13}C-NMR, indicating that dynamical interchange is averaging their environments on the NMR timescale. Three signals were found in the ^{31}P-NMR spectrum. The first one, the most intense, was a sharp singlet at 22.17 ppm, and corresponds to a major isomer in which both ends of the dppm ligand are bound to Ru atoms, and are equivalent. The second one was a doublet at 20.68 ppm, with coupling constant $J_{P-P} = 37.1$ Hz. The third one was a triplet of doublets centred at −13.44 ppm, with coupling constants $J_{P-P} = 36.8$ Hz and $J_{Pt-P} = 3706$ Hz, indicating that it is a platinum-bound phosphorus. The fact that these two signals are coupled together suggests that they arise from a minor isomer, in which one phosphorus is bound to a ruthenium atom (giving the signal at 20.68 ppm), and the other is linked to a platinum atom (giving the signal at −13.44 ppm). Possible structures for both isomers are illustrated in Fig. 6. The compound $[Ru_5C(CO)_{14}Pt(dppe)]$ **13** was obtained in a very similar fashion by substitution of the COD ligand in $[Ru_5C(CO)_{14}Pt(COD)]$ **1** by dppe.[14] However, in $[Ru_5C(CO)_{14}Pt(dppe)]$ **13**, the dppe ligand is chelating the platinum atom, and $[Ru_5C(CO)_{14}Pt(dppe)]$ **13** is the product of direct substitution of the bidentate COD ligand by the bidentate diphosphine ligand.

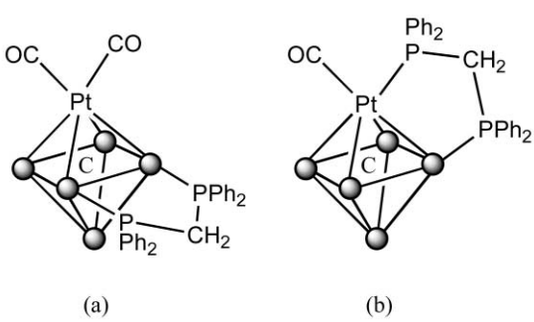

Fig. 6 Possible structures for $[Ru_5C(CO)_{14}Pt(\mu\text{-dppm})]$ **10**: (a) major isomer, (b) minor isomer. Shaded circles represent Ru. The carbonyl ligands attached to ruthenium atoms are omitted for clarity.

Table 1 Selected bond lengths (Å) and angles (°) for $[Ru_5C(CO)_{14}Pt(\mu\text{-dppm})]$ **10**

Ru(1)–P(1)	2.3533(14)	Ru(2)–Ru(5)	2.9206(6)
Ru(2)–P(2)	2.3141(14)	Ru(3)–Ru(5)	2.9257(6)
P(1)–C(27)	1.832(5)	Ru(4)–Ru(5)	2.8310(6)
P(2)–C(27)	1.811(5)	Ru(1)–Ru(2)	2.9603(6)
Ru(1)–Pt(1)	2.9275(5)	Ru(2)–Ru(3)	2.8787(6)
Ru(2)–Pt(1)	2.9361(5)	Ru(3)–Ru(4)	2.9205(6)
Ru(3)–Pt(1)	2.7967(5)	Ru(4)–Ru(1)	2.9024(6)
Ru(4)–Pt(1)	2.9540(5)	Pt(1)–C(0)	2.053(5)
Ru(1)–Ru(5)	2.9261(6)	C–O (mean)	1.141(3)
Ru(1)–P(1)–C(27)	111.97(18)	P(1)–Ru(1)–Ru(2)	92.87(4)
Ru(2)–P(2)–C(27)	111.72(19)	P(2)–Ru(2)–Ru(1)	84.08(4)
P(1)–C(27)–P(2)	110.7(3)	Pt(1)–C(0)–Ru(5)	175.9(3)

This difference in behaviour must be due to the different separation of the two P atoms (bite) in dppm compared to dppe. Chelating dppm is strained and a bridging bonding mode is favoured. However, the hypothetic cluster $[Ru_5C(CO)_{14}Pt(dppm)]$ **14**, in which the ligand dppm is chelating the platinum atom, must constitute an intermediate for the structures observed for **10**.

Single crystals of **10** were grown, and the structure shown in Fig. 7 was obtained by X-ray crystallography. Selected bond lengths and angles are presented in Table 1. The molecule consists of a Ru_5Pt octahedron with a dppm ligand bridging a Ru–Ru edge. This corresponds to the major isomer observed in solution (see Fig. 6(a)). The octahedral geometry of the cluster core is in accord with the PSEPT rules for compound **10** (86 electron count). The platinum atom bears one terminal carbonyl ligand and shares one bridging CO with a neighbouring ruthenium (Ru(3)). All the other CO ligands are terminally bound to ruthenium atoms and are almost linear. The octahedron does not display any particular distortion, with the carbide atom lying in its centre. The Ru–Ru bond lengths (range: 2.8310(6) Å–2.9603(6) Å) are longer on average than in $[Ru_5C(CO)_{15}]$ **6** and derivatives,[10] and the Ru–Ru edge supporting the bridging dppm (Ru(1)–Ru(2)) is the longest of all. The Ru–Pt bond distances range from 2.7967(5) to 2.9540(5) Å, which is similar to the values found in other octahedral Ru_5Pt clusters.[3,4] The shortest Ru–Pt distance (Ru(3)–Pt(1)) is associated with the bridging CO ligand. The Ru–P distances to the dppm ligand appear to be normal. The Ru–P bonds are almost perpendicular to the Ru–Ru edge bridged by the diphosphine unit, as would have been expected (see angles: P(1)–Ru(1)–Ru(2) = 92.87(4) and P(2)–Ru(2)–Ru(1) = 84.08(4)°). The two P atoms and the carbon of the CH_2 unit linking them are all tetrahedral. However, all the angles C–P–C are smaller than the C–P–Ru angles, which is probably due to the steric constraints of the cluster core.

The third product, $[Ru_5C(CO)_{11}Pt(CO)(dppm)_2]$ **11**, was obtained in 8.7% yield. It was formulated on the basis of satisfactory elemental analysis. Carbonyl stretching frequencies attributable to both terminal and bridging CO ligands were found in its IR spectrum. The possibility of this compound being $[Ru_5C(CO)_{13}(dppm)]$ **12** was discarded on the basis of an IR spectrum taken in cyclohexane solution.[11] The ^{1}H- and ^{13}C-NMR spectra were consistent with the suggested formulation. Both dppm ligands in **11** were found to be equivalent in solution: a single peak at 16.78 ppm was found in the ^{31}P-NMR spectrum. Single crystals of $[Ru_5C(CO)_{11}Pt(CO)(dppm)_2]$ **11** were grown, and an X-ray diffraction analysis undertaken. The structure obtained is shown in Fig. 8 and selected bond lengths and angles are reported in Table 2.

The asymmetric unit of the structure contains two independent but structurally similar molecules. The compound $[Ru_5C(CO)_{11}Pt(CO)(dppm)_2]$ **11** consists of a Ru_5Pt octahedron with two dppm ligands bound symmetrically to the "equatorial" ruthenium atoms (if the Pt is defined to be occupying an "apical" position). The platinum bears a terminal CO ligand. In

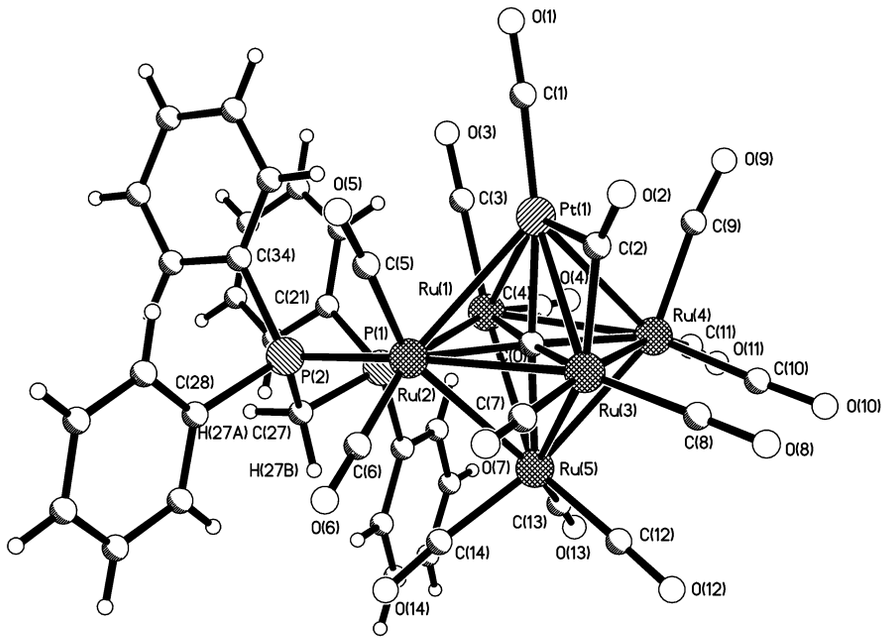

Fig. 7 Molecular structure of $[Ru_5C(CO)_{14}Pt(\mu\text{-dppm})]$ **10**, showing the atom labelling scheme.

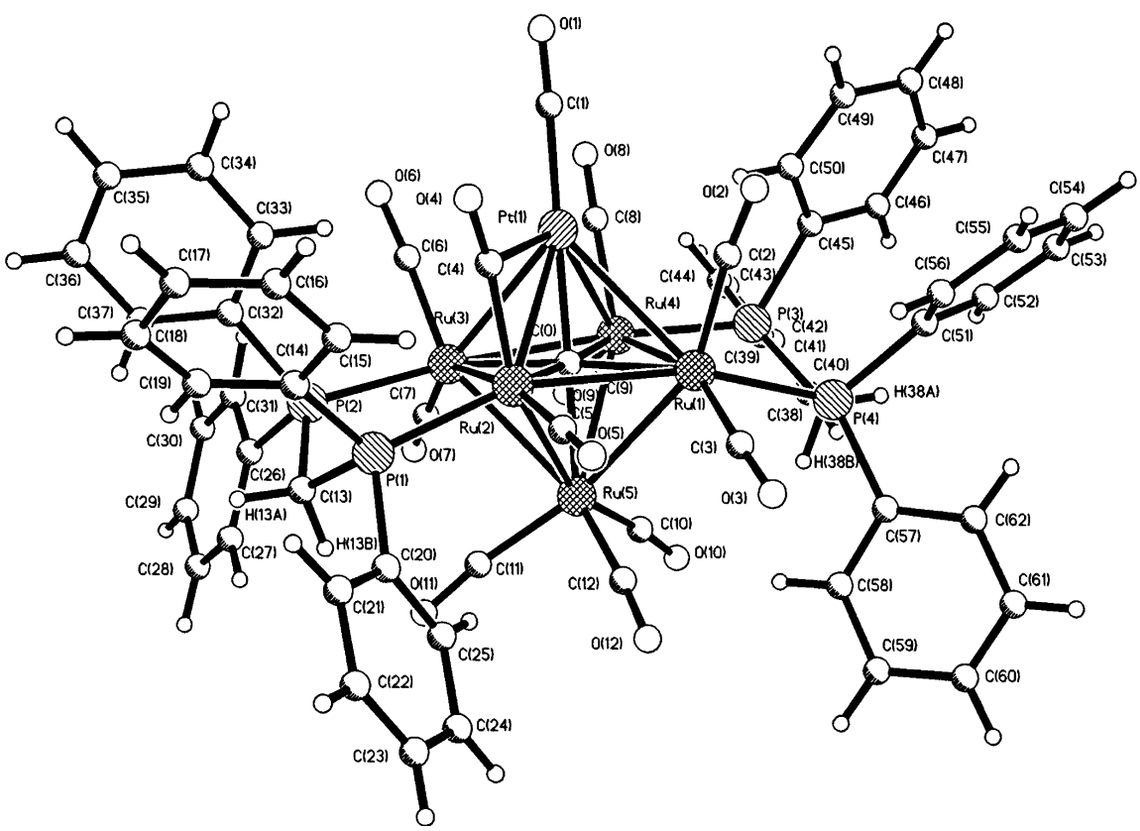

Fig. 8 Molecular structure of $[Ru_5C(CO)_{11}Pt(CO)(dppm)_2]$ **11**, showing the atom labelling scheme.

addition, a semi-bridging carbonyl (C(4)O(4)) is present on the Ru(2)–Pt edge (the angle Ru(2)–C(4)–O(4) is smaller than 180° {162.3(8)° in molecule 1 and 159.7(9)° in molecule 2}, indicating interaction with the Pt atom). However, the distance Pt–C(4)O(4) is very long (2.462(10) Å in molecule 1 and 2.410(10) Å in molecule 2), and cannot really be considered as a bond. All the other CO ligands are terminally bound to Ru atoms and almost linear. The carbonyl on the Pt atom is also linear: the angle Pt(1)–C(1)–O(1) is 177.8(10)° in molecule 1 and 173.3(10)° in molecule 2. The Ru_5Pt octahedron is unchanged, with the carbide atom lying nearly perfectly in the centre. The Ru–Ru bonds range between 2.8566(10) and 2.9801(11) Å in molecule 1, and between 2.8403(10) and 2.9796(10) Å in molecule 2. This is longer than the values reported for $[Ru_5C(CO)_{15}]$ **6**,[10] $[Ru_5C(CO)_{13}(dppm)]$ **12**,[11] $[Ru_5C(CO)_{14}Pt(dppe)]$ **13** [14] and $[Ru_5C(CO)_{14}Pt(COD)]$ **1**,[3] and even slightly longer on average than in compound **10**. It must be an effect of the number of phosphine ligands on the cluster. The Ru(basal)–Ru(basal) bonds of the Ru_5 pyramid are slightly longer than the Ru(apical)–Ru(basal) bonds, as observed previously in $[Ru_5C(CO)_{15}]$ **6** and its derivatives. The Ru–Ru bonds bridged by dppm ligands seem to be associated with the greatest distances, an effect which had not been noticed in the case of $[Ru_5C(CO)_{13}(dppm)]$ **12**,[11] but was observed for compound **10**

Table 2 Selected bond lengths (Å) and angles (°) for $[Ru_5C(CO)_{11}Pt(CO)(dppm)_2]$ **11**

	Molecule 1	Molecule 2		Molecule 1	Molecule 2
Ru(1)–Pt(1)	2.9751(8)	2.8843(8)	Ru(2)–P(1)	2.343(2)	2.341(2)
Ru(2)–Pt(1)	2.8445(8)	2.8587(8)	Ru(3)–P(2)	2.331(2)	2.326(2)
Ru(3)–Pt(1)	2.9246(8)	2.8972(9)	Ru(4)–P(3)	2.322(2)	2.327(2)
Ru(4)–Pt(1)	2.8695(9)	2.9659(9)	Ru(1)–P(4)	2.350(3)	2.325(2)
Pt(1)–C(1)	1.860(11)	1.836(12)	P(1)–C(13)	1.843(9)	1.839(9)
Ru(5)–Ru(1)	2.8730(11)	2.9012(11)	P(2)–C(13)	1.846(8)	1.821(9)
Ru(5)–Ru(2)	2.9801(11)	2.9026(11)	P(4)–C(38)	1.833(9)	1.843(8)
Ru(5)–Ru(3)	2.8708(10)	2.9488(10)	P(3)–C(38)	1.828(9)	1.824(8)
Ru(5)–Ru(4)	2.9304(10)	2.8816(10)	Pt(1)–C(4)	2.462(10)	2.410(10)
Ru(1)–Ru(2)	2.9238(10)	2.9340(10)	Ru(2)–C(4)	1.900(10)	1.929(11)
Ru(2)–Ru(3)	2.9574(10)	2.9730(10)	Pt(1)–C(0)	2.028(8)	2.023(9)
Ru(3)–Ru(4)	2.8566(10)	2.8403(10)	Ru(5)–C(0)	2.063(8)	2.047(9)
Ru(1)–Ru(4)	2.9691(10)	2.9796(10)	C–O (mean)	1.152(4)	1.151(3)

	Molecule 1	Molecule 2
Pt(1)–C(1)–O(1)	177.8(10)	173.3(10)
Pt(1)–C(0)–Ru(5)	177.6(5)	177.9(5)
Ru(2)–C(4)–O(4)	162.3(8)	159.7(9)
P(1)–Ru(2)–Ru(3)	93.04(6)	93.00(6)
P(2)–Ru(3)–Ru(2)	87.68(7)	83.45(6)
P(4)–Ru(1)–Ru(4)	92.32(7)	93.26(6)
P(3)–Ru(4)–Ru(1)	86.67(7)	86.38(6)
P(1)–C(13)–P(2)	109.4(4)	109.5(5)
P(3)–C(38)–P(4)	110.1(5)	112.0(4)
Ru(2)–P(1)–C(13)	113.7(3)	112.3(3)
Ru(3)–P(2)–C(13)	114.9(3)	111.4(3)
Ru(4)–P(3)–C(38)	112.6(3)	115.5(3)
Ru(1)–P(4)–C(38)	113.4(3)	114.8(3)

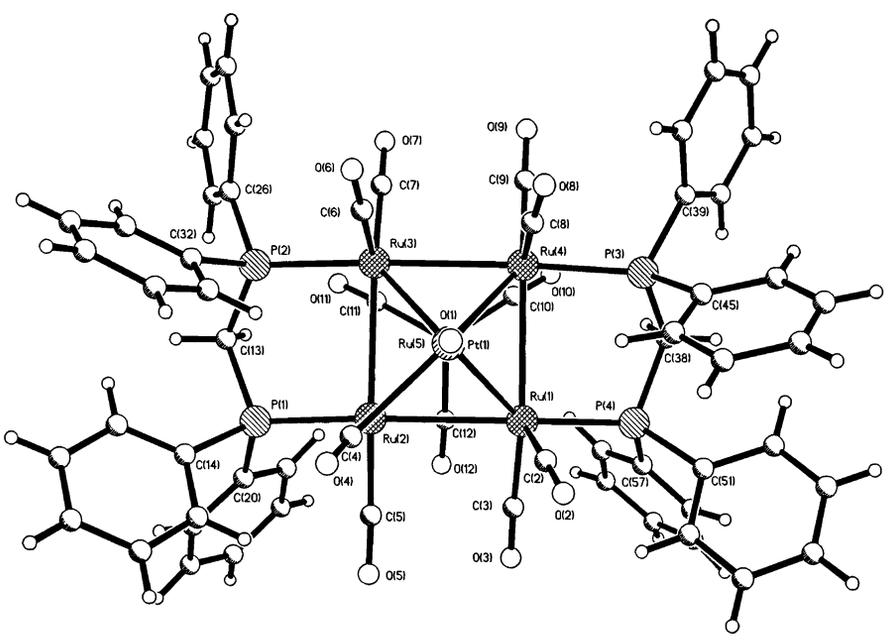

Fig. 9 Top view of the molecular structure of $[Ru_5C(CO)_{11}Pt(CO)(dppm)_2]$ **11**.

and $[Ru_6C(CO)_{15}dppm]$ **15**.[15] The Ru–Pt bond distances vary in the range 2.8445(8)–2.9751(8) Å (molecule 1) and 2.8587(8)–2.9659(9) Å (molecule 2). This is within the range reported for $[Ru_5CPt(CO)_{16}]$ **3** [4] and $[Ru_5C(CO)_{14}Pt(COD)]$ **1**,[3] but are slightly longer than a mean Ru–Pt distance calculated over all the Ru–Pt compounds characterised by X-ray diffraction (2.789 Å). In $[Ru_5C(CO)_{14}Pt(dppe)]$ **13**, the Ru–Pt distances were even longer, which had been attributed to the steric requirement of the chelating dppe ligand.[14] The shortest Ru–Pt bond in $[Ru_5C(CO)_{11}Pt(CO)(dppm)_2]$ **11** is associated with the semi-bridging CO ligand. The two dppm ligands are bridging Ru–Ru edges symmetrically on opposite sides of the octahedron (see Fig. 9, displaying a top view of the molecular structure). They occupy equatorial sites on each Ru atom, in contrast with $[Ru_5C(CO)_{13}(dppm)]$ **12**,[11] where the diphosphine ligand occupies axial sites on the Ru atoms. This confers a pseudo two-fold axis of symmetry to the molecule, passing through the Pt and the central carbide atoms. The four phosphorus atoms all sit slightly underneath the plane formed by the four Ru atoms to which they are linked (see Fig. 10, showing a different view (side-on) of the molecule). The P–C bonds to the two central CH_2 of the dppm units are all directed away from the side of the cluster containing the Pt atom. The angles at the CH_2 groups are ideal for sp^3-hybridised carbons. The four P atoms are tetrahedral, with angles ranging from 100.4(4) to 118.8(3)° in molecule 1, and from 99.4(4) to 120.5(3)° in molecule 2. However, the C–P–C angles (~105°) are on average smaller than the C–P–Ru angles (~115°), as in compound **10**. The Ru–P

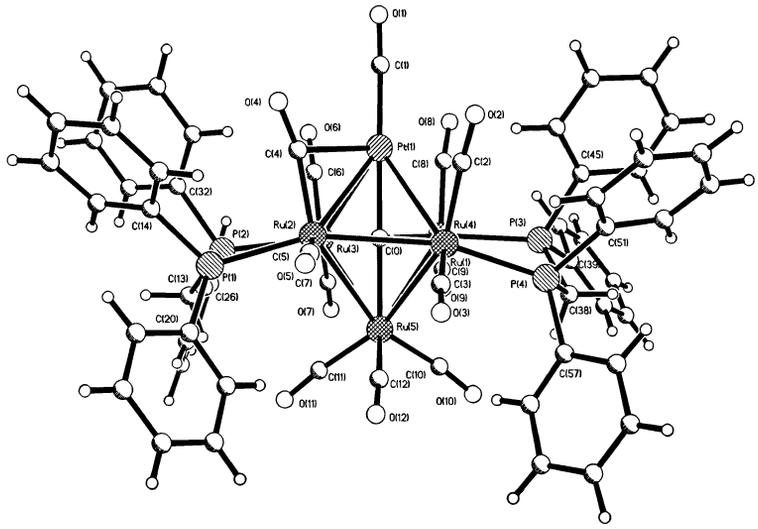

Fig. 10 Side-on view of the molecular structure of $[Ru_5C(CO)_{11}Pt(CO)(dppm)_2]$ **11**.

distances [2.322(2)–2.350(3) Å] are within the range previously observed, such as 2.376(2) Å in $[Ru_6C(CO)_{16}PPh_3]$ **16**,[16] 2.359(3) Å in $[Ru_6C(CO)_{16}(PPh_2Et)]$ **17**,[17] or 2.312(4)–2.320(4) Å in $[Ru_5C(CO)_{13}(dppm)]$ **12**.[11] The total electron count for **11** is 86 electrons, which is in line with that predicted by the PSEPT rules for a *closo* octahedral geometry.

The mechanism of formation of $[Ru_5C(CO)_{11}Pt(CO)(dppm)_2]$ **11** is uncertain, but the isomers observed for $[Ru_5C(CO)_{14}Pt(\mu\text{-dppm})]$ **10** might give some indication. As previously discussed, the first step in the reaction of dppm with $[Ru_5C(CO)_{14}Pt(COD)]$ **1** is probably substitution of the COD for a chelating dppm. Due to the strain experienced by a chelating dppm, the diphosphine migrates to a bridging bonding mode, producing the minor isomer of $[Ru_5C(CO)_{14}Pt(\mu\text{-dppm})]$ **10b** shown in Fig. 6(b). The dppm ligand migrates further to bridge two ruthenium atoms, producing the major isomer of $[Ru_5C(CO)_{14}Pt(\mu\text{-dppm})]$ **10a** shown in Fig. 6(a), and observed in the solid state. A second dppm unit adds to the cluster, probably *via* a short-lived intermediate in which it is chelating the Pt atom. Finally, the second dppm ligand migrates from the platinum to become a bridge between two Ru atoms, as observed in the solid state structure of $[Ru_5C(CO)_{11}Pt(CO)(dppm)_2]$ **11**. This mechanism is suggested in relation with the general observation that phosphine ligands tend to migrate from the platinum to the ruthenium atoms in Ru–Pt mixed-metal clusters.[3,31] The proposal is summarised in Fig. 11. In this mechanism, the platinum atom behaves as an "entry port" for the incoming diphosphine ligands.

2.2. Attempts to substitute the COD ligand in $[Ru_6C(CO)_{16}Pt(COD)]$ 2. $[Ru_6C(CO)_{16}Pt(COD)]$ **2** was reacted with triphenylphosphine in dichloromethane at room temperature. Two compounds were isolated from the reaction mixture. The first one was identified as the known $[Ru_6C(CO)_{16}PPh_3]$ **16** on the basis of its IR spectrum,[17] and mass spectrometry results. The second product was formulated as $[Ru_6C(CO)_{15}(PPh_3)_2]$ **18** on the basis of its IR spectrum only, by comparison with data from the literature.[17] The molecular peak could not be obtained by mass spectrometry: instead a peak at *m*/*z* 1161, corresponding to the fragment $[Ru_6C(CO)_{10}(PPh_3)]$, was observed, which was followed by the loss of 10 CO ligands, and consequently one Ph ligand. The formation of these two species involves replacement of the Pt(COD) unit in $[Ru_6C(CO)_{16}Pt(COD)]$ **2** by PPh_3 to give **16**, followed by substitution of one CO ligand for a second PPh_3 to lead to **18**. These results parallel what had been obtained with $[Ru_5C(CO)_{14}Pt(COD)]$ **1** in the reaction with excess triphenylphosphine: the loss of the Pt atom is accompanied by formation of bis(phosphine) derivatives. Both compounds **16** and **18** have a total electron count of 86, and thus the PSEPT rules predict octahedral metal core geometries for both (*i.e.* an unchanged arrangement of Ru atoms).

Table 3 Selected bond lengths (Å) and angles (°) for $[Ru_6C(CO)_{13}(dppm)_2]$ **19**

Ru(1)–P(1)	2.324(2)	Ru(4)–Ru(5)	2.9025(9)
Ru(2)–P(2)	2.308(2)	Ru(1)–Ru(6)	2.9313(8)
Ru(6)–P(3)	2.310(2)	Ru(2)–Ru(6)	2.9612(9)
Ru(3)–P(4)	2.3218(19)	Ru(3)–Ru(6)	2.9479(9)
P(1)–C(26)	1.832(8)	Ru(4)–Ru(6)	3.0082(8)
P(2)–C(26)	1.832(7)	Ru(1)–Ru(2)	3.0066(8)
P(3)–C(51)	1.844(7)	Ru(2)–Ru(3)	2.9704(9)
P(4)–C(51)	1.837(7)	Ru(3)–Ru(4)	2.8469(8)
Ru(1)–Ru(5)	2.9142(9)	Ru(4)–Ru(1)	2.8108(9)
Ru(2)–Ru(5)	2.8172(8)	Ru–C(100) (mean)	2.062(6)
Ru(3)–Ru(5)	2.8691(8)	C–O (mean)	1.149(3)
Ru(1)–P(1)–C(26)	113.8(3)	P(2)–Ru(2)–Ru(5)	117.29(5)
Ru(2)–P(2)–C(26)	110.8(3)	P(3)–Ru(6)–Ru(4)	87.10(5)
Ru(6)–P(3)–C(51)	115.5(2)	P(4)–Ru(3)–Ru(5)	167.38(6)
Ru(3)–P(4)–C(51)	114.2(2)	P(1)–C(26)–P(2)	110.1(4)
P(1)–Ru(1)–Ru(5)	111.57(6)	P(3)–C(51)–P(4)	113.3(4)

$[Ru_6C(CO)_{16}Pt(COD)]$ **2** was then reacted with dppm in dichloromethane under refluxing conditions. Four compounds could be isolated by thin-layer chromatography. These were formulated as $[Ru_6C(CO)_{15}(dppm)]$ **15**, $[Ru_6C(CO)_{13}(dppm)_2]$ **19**, $[Ru_6C(CO)_{15}Pt_2(dppm)]$ **20**, and $[Ru_6C(CO)_{16}Pt_3(dppm)_2]$ **21**. The compound $[Ru_6C(CO)_{15}(dppm)]$ **15** was identified on the basis of its IR, mass and NMR spectra, by comparison with data from the literature.[15] Crystals of $[Ru_6C(CO)_{15}(dppm)]$ **15** suitable for X-ray structure determination were obtained, and the unit cell parameters also fitted with the literature data.[15] The cluster $[Ru_6C(CO)_{15}(dppm)]$ had been shown to display an octahedral cluster core,[15] in accord with the PSEPT rules for the 86 electron count of **15**. The second product, by order of elution, was $[Ru_6C(CO)_{13}(dppm)_2]$ **19**. Carbonyl ligands both terminally bound and in a bridging bonding mode were identified by IR spectroscopy. The molecular peak was observed at *m*/*z* 1751, and was followed by CO ligand losses. Crystals suitable for X-ray diffraction analysis were grown. The structure obtained is shown in Fig. 12, and selected bond lengths and angles are reported in Table 3.

The molecule consists of a Ru_6 carbide octahedron with two dppm ligands bridging Ru–Ru edges. If one dppm is said to be linked to two "equatorial" ruthenium atoms, then the other might be described as linked to a Ru"apical"–Ru"equatorial" edge. This is in contrast with $[Ru_5C(CO)_{11}Pt(CO)(dppm)_2]$ **11**,

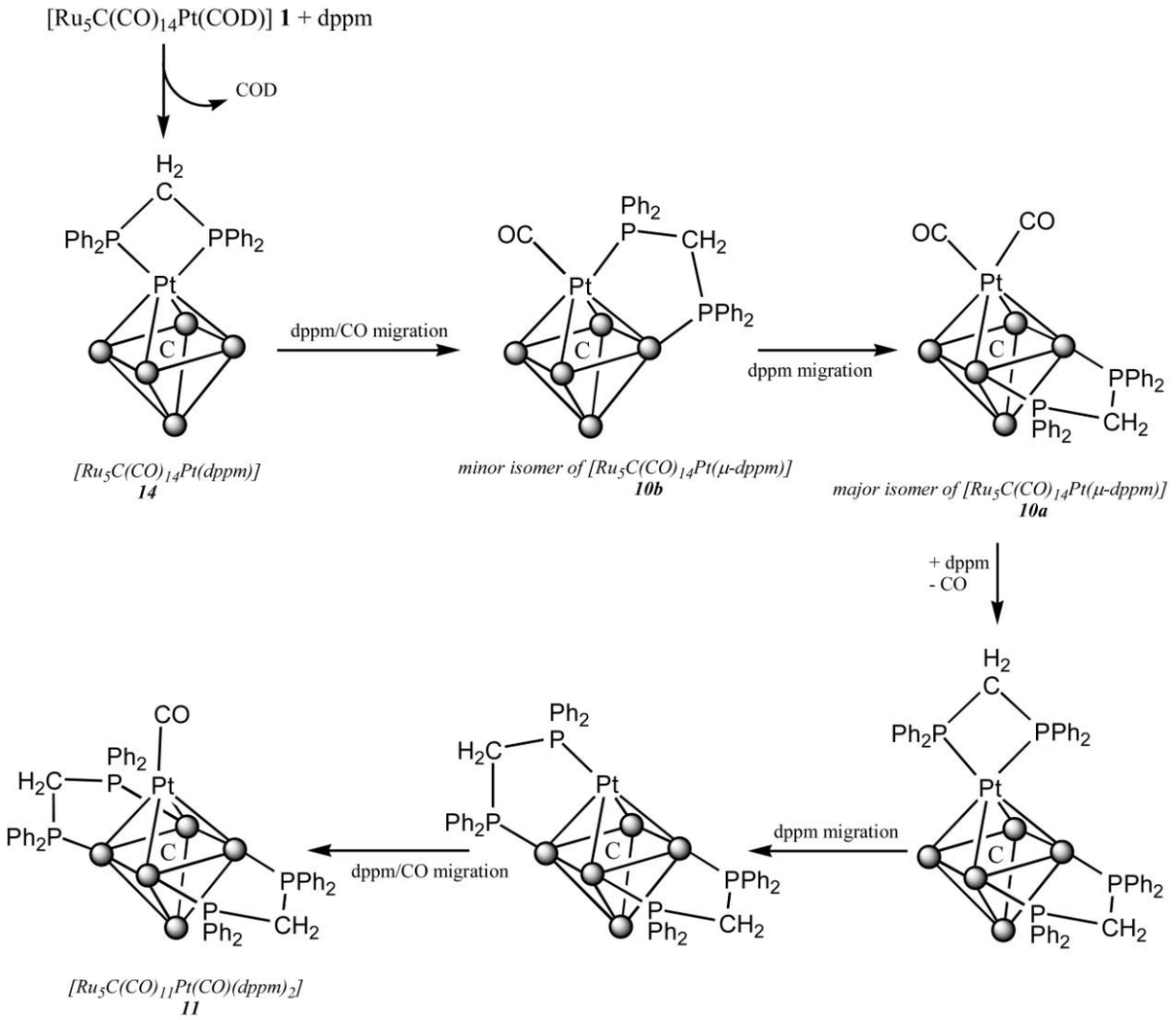

Fig. 11 Proposed mechanism of formation for $[Ru_5C(CO)_{11}Pt(CO)(dppm)_2]$ **11**. Shaded circles represent Ru. The carbonyl ligands attached to ruthenium atoms are omitted for clarity.

where the two dppm ligands were bound to four Ru atoms comprised in the same plane (*vide supra*). However, both clusters **11** and **19** have a total electron count of 86, which, according to the PSEPT rules, leads to an octahedral metal core. This is indeed the case in both compounds, but is accompanied by non-rigidity in the ligand arrangement around that fixed metal core, as is often the case in cluster chemistry. Eleven carbonyl ligands are terminally bound to Ru atoms. Two CO ligands are bridging Ru"apical"–Ru"equatorial" edges, on opposite sides of the octahedron. The octahedron is unchanged when compared to $[Ru_6C(CO)_{17}]$ **5**. The Ru–Ru bonds range from 2.8108(9) to 3.0082(8) Å, which is similar to the mean value of 2.90(2) Å found in $[Ru_6C(CO)_{17}]$ **5** itself,[18] or the range 2.844(1)–2.989(1) Å found in $[Ru_6C(CO)_{15}dppm]$ **15**.[15] The Ru–Ru bonds bridged by the dppm ligands are amongst the longest found in the molecule, but are not associated with the greatest value, in contrast to $[Ru_6C(CO)_{15}(dppm)]$ **15**.[15] This is probably due to the fact that the effects of the two bridging diphosphines on opposite sides of the octahedron counterbalance each other. Similarly, the Ru–Ru bonds bridged by CO ligands are amongst the smallest bond distances, but not strictly the shortest. The angles at the P atoms range from 98.0(3) to 120.9(3)°, which gives them a tetrahedral environment. The angles C–P–Ru (~115°) are systematically larger than the angles C–P–C (~103°), a trend that had already been noticed for compounds **10** and **11** (*vide supra*). The two CH_2 groupings of the dppm ligands are normal sp^3 hybridised carbon atoms. However, the angles P–C–P are more open than the angles H–C–H or P–C–H. This is probably due to the strain associated with the five-membered rings Ru–Ru–P–C–P formed by the bridging ligands. The distances Ru–P range from 2.308(2) to 2.324(2) Å, which is slightly shorter on average than the values found for $[Ru_6C(CO)_{15}(dppm)]$ **15** (2.333(3) and 2.347(3) Å),[15] $[Ru_6C(CO)_{16}PPh_3]$ **16** (2.376(2) Å),[16] $[Ru_6C(CO)_{16}(PPh_2Et)]$ **17** (2.359(3) Å) [17] and $[Ru_5C(CO)_{11}Pt(CO)(dppm)_2]$ **11** (2.322(2)–2.350(3) Å), but similar to the values reported for $[Ru_5C(CO)_{13}(dppm)]$ **12** (2.312(4)–2.320(4) Å).[11]

The third product, $[Ru_6C(CO)_{15}Pt_2(dppm)]$ **20**, was only characterised by IR spectroscopy and mass spectrometry, due to the very low yield in which it was isolated. Its IR spectrum displayed bands attributable to terminal CO ligands only. The molecular peak was found at *m*/*z* 1818, and was followed by CO loss peaks.

The fourth product obtained, $[Ru_6C(CO)_{16}Pt_3(dppm)_2]$ **21**, displayed peaks attributable to both terminal and bridging CO ligands in its IR spectrum. Characterisation by mass spectrometry allowed the observation of the molecular peak at *m*/*z* 2420, together with CO loss peaks. Crystals suitable for X-ray diffraction structure determination were grown. The structure obtained is shown in Fig. 13. Selected bond lengths and angles are reported in Table 4.

The asymmetric unit of the structure contains two independent but structurally similar molecules. The molecular structure consists of a $[Ru_6C(CO)_{16}]$ octahedron linked to a triangular Pt_3 unit bearing two bridging dppm ligands. The octahedral arrangement of the six ruthenium atoms is not unusual, with all

Table 4 Selected bond lengths (Å) and angles (°) for $[Ru_6C(CO)_{16}Pt_3(dppm)_2]$ **21**

Molecule 1		Molecule 2		Molecule 1		Molecule 2	
Pt(1)–Pt(2)	2.9090(14)	Pt(4)–Pt(5)	2.8877(13)	Ru(4)–Ru(6)	2.926(3)	Ru(10)–Ru(9)	2.935(3)
Pt(2)–Pt(3)	2.6227(14)	Pt(6)–Pt(4)	2.6240(12)	Ru(5)–Ru(6)	2.859(3)	Ru(11)–Ru(9)	2.856(3)
Pt(3)–Pt(1)	2.6078(13)	Pt(5)–Pt(6)	2.6191(14)	Ru(1)–Ru(2)	3.142(3)	Ru(7)–Ru(8)	3.124(3)
Ru(1)–Pt(1)	2.713(2)	Ru(7)–Pt(5)	2.693(2)	Ru(2)–Ru(4)	2.763(3)	Ru(8)–Ru(10)	2.764(3)
Ru(2)–Pt(1)	2.775(2)	Ru(8)–Pt(5)	2.775(2)	Ru(4)–Ru(5)	2.850(3)	Ru(10)–Ru(11)	2.882(3)
Ru(3)–Pt(1)	3.081(2)	Ru(12)–Pt(5)	3.136(2)	Ru(1)–Ru(5)	2.913(3)	Ru(7)–Ru(11)	2.904(3)
Ru(1)–Pt(2)	2.718(2)	Ru(7)–Pt(4)	2.727(2)	Pt(1)–P(1)	2.246(8)	Pt(5)–P(7)	2.246(6)
Ru(2)–Pt(2)	2.745(2)	Ru(8)–Pt(4)	2.759(2)	Pt(3)–P(2)	2.245(7)	Pt(6)–P(8)	2.268(6)
Ru(6)–Pt(2)	3.187(3)	Ru(9)–Pt(4)	3.188(2)	Pt(3)–P(4)	2.256(6)	Pt(6)–P(6)	2.283(7)
Ru(1)–Ru(3)	2.882(3)	Ru(7)–Ru(12)	2.872(3)	Pt(2)–P(3)	2.249(6)	Pt(4)–P(5)	2.229(7)
Ru(2)–Ru(3)	2.988(3)	Ru(8)–Ru(12)	2.956(3)	P(1)–C(29)	1.87(3)	P(7)–C(120)	1.82(3)
Ru(4)–Ru(3)	2.930(3)	Ru(10)–Ru(12)	2.929(3)	P(2)–C(29)	1.83(3)	P(8)–C(120)	1.84(3)
Ru(5)–Ru(3)	2.853(3)	Ru(11)–Ru(12)	2.859(3)	P(3)–C(54)	1.85(3)	P(5)–C(95)	1.82(3)
Ru(1)–Ru(6)	2.864(3)	Ru(7)–Ru(9)	2.870(3)	P(4)–C(54)	1.83(3)	P(6)–C(95)	1.86(3)
Ru(2)–Ru(6)	2.955(3)	Ru(8)–Ru(9)	2.980(3)	C–O (mean)	1.169(8)	C–O (mean)	1.163(8)

Molecule 1		Molecule 2	
Pt(2)–Pt(1)–Pt(3)	56.45(3)	Pt(4)–Pt(5)–Pt(6)	56.66(3)
Pt(1)–Pt(2)–Pt(3)	55.96(3)	Pt(5)–Pt(4)–Pt(6)	56.50(3)
Pt(1)–Pt(3)–Pt(2)	67.58(4)	Pt(5)–Pt(6)–Pt(4)	66.84(4)
P(2)–Pt(3)–Pt(1)	95.19(17)	P(8)–Pt(6)–Pt(5)	94.86(17)
P(1)–Pt(1)–Pt(3)	88.78(17)	P(7)–Pt(5)–Pt(6)	88.88(18)
P(3)–Pt(2)–Pt(3)	90.72(18)	P(5)–Pt(4)–Pt(6)	90.43(15)
P(4)–Pt(3)–Pt(2)	96.99(19)	P(6)–Pt(6)–Pt(4)	97.44(15)
P(1)–C(29)–P(2)	109.6(14)	P(7)–C(120)–P(8)	111.2(14)
P(3)–C(54)–P(4)	109.9(14)	P(5)–C(95)–P(6)	110.7(14)

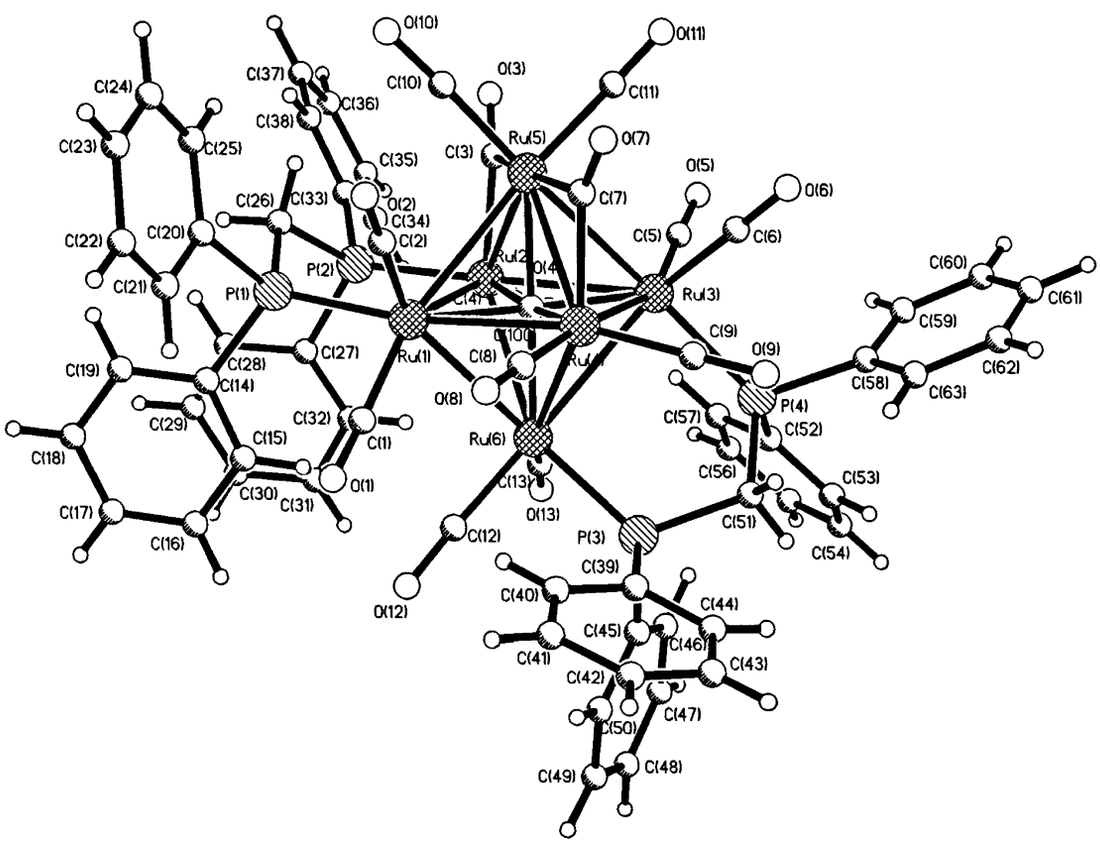

Fig. 12 Molecular structure of $[Ru_6C(CO)_{13}(dppm)_2]$ **19**, showing the atom labelling scheme.

its features shared by other derivatives of the hexaruthenium carbide cluster $[Ru_6C(CO)_{17}]$ **5**. Three carbonyl ligands are bridging Ru–Ru bonds, and two are bridging Ru–Pt bonds, while all the other carbonyls are terminally bound to ruthenium atoms. The Ru–Ru bond lengths vary from 2.763(3) to 3.142(3) Å in molecule 1, and from 2.764(3) to 3.124(3) Å in molecule 2. This is very similar to the distances 2.827(5)–3.034(5) Å found in $[Ru_6C(CO)_{17}]$ **5** itself,[18] but spans a slightly wider range of values. This is probably due to the contradictory effects of bridging carbonyls and the platinum fragment. Indeed, the Ru–Ru bonds spanned by bridging CO ligands are amongst the shortest, whereas the Ru–Ru bond directly bridged by the Pt triangle is by far the longest (Ru(1)–Ru(2) = 3.142(3) Å in molecule 1). The Ru–Pt bonds can be classified in two categories: the four bonds to Ru(1) and Ru(2) are short, while the two bonds to Ru(3) and Ru(6) are long. The "short" bonds are close to the

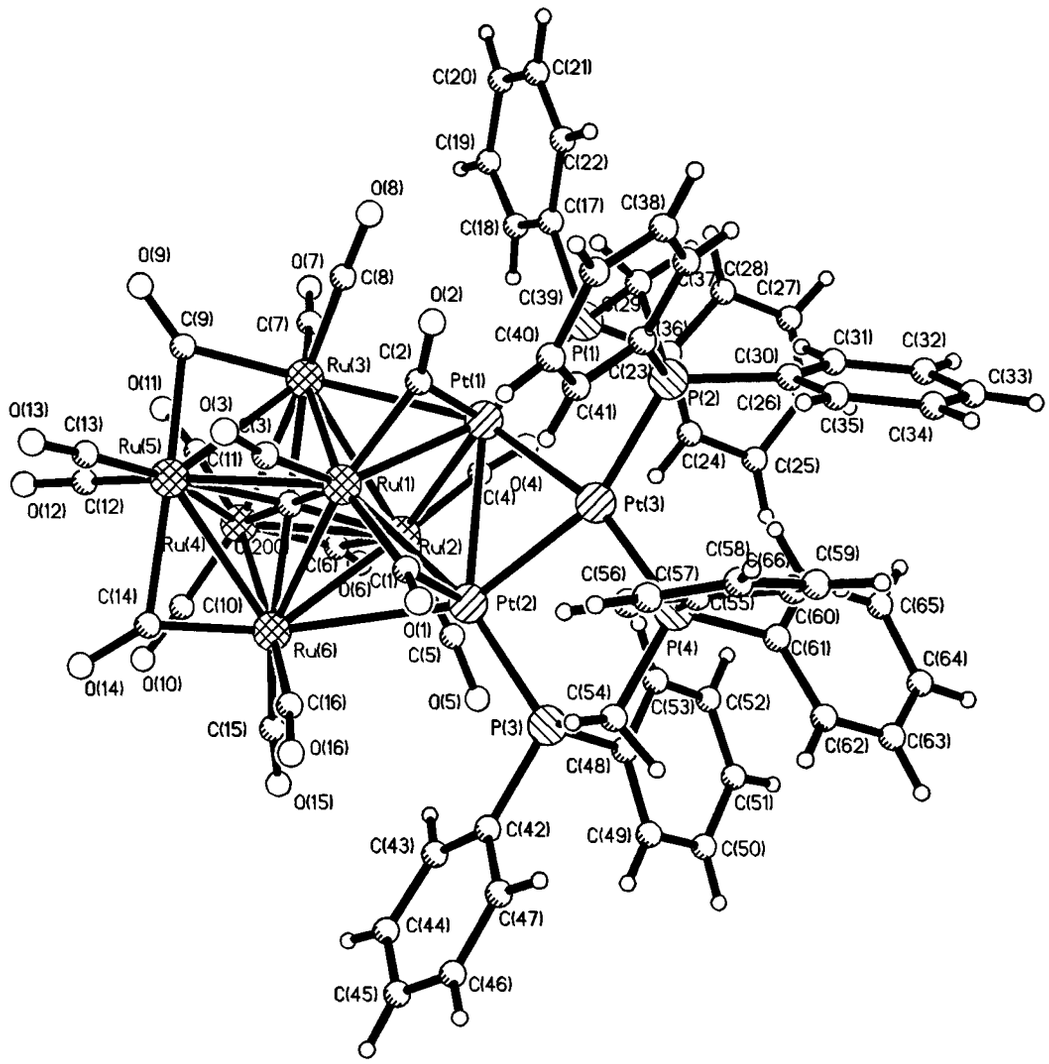

Fig. 13 Molecular structure $[Ru_6C(CO)_{16}Pt_3(dppm)_2]$ **21**, showing the atom labelling scheme.

mean value of 2.789 Å calculated over the whole range of compounds containing Ru–Pt bonds that have been characterised by X-ray crystallography. It is also very similar to the values of Ru–Pt bonds found in $[Ru_6C(CO)_{16}Pt(COD)]$ **2**,[3] $[Ru_6C(CO)_{15}(Pt(COD))_2]$ **23**[3] and $[\{Ru_6C(CO)_{16}\}_2Pt(MeCN)_2]$ **24**.[19] The "long" bonds (ranging from 3.081(2) to 3.188(2) Å), however, are outside the range of bond lengths observed in those three compounds and are reaching the limit of distances that can be considered as bonding between a Pt and a Ru atom. The Pt–Pt bonds vary in length, with the distance between Pt(1) and Pt(2), which are bound to ruthenium, being longer. The Pt(1)–Pt(3) and Pt(2)–Pt(3) bond lengths are very similar to the values (~2.6 Å) reported for the few known Ru–Pt high nuclearity mixed-metal clusters containing Pt triangles, such as: $[Pt_4Ru_5(CO)_{20}(COD)]$,[20] $[Pt_5Ru_5(CO)_{18}(COD)_2(\mu_3\text{-}H)_2]$ [21] or the layer-segregated $[Ru_6Pt_3(CO)_{21}(\mu\text{-}CO)(\mu\text{-}H)_2]$,[22] $[Ru_6Pt_3(CO)_{21}(\mu\text{-}H)_3(\mu_3\text{-}H)]$, $[Ru_6Pt_3(CO)_{20}(\mu_3\text{-}PhC_2Ph)(\mu_3\text{-}H)(\mu\text{-}H)]$,[23] and $[Ru_6Pt_3(CO)_{21}(\mu\text{-}PhCC(H)Ph)(\mu\text{-}H)]$.[24] The arrangement of metal atoms in $[Ru_6C(CO)_{16}Pt_3(dppm)_2]$ **21** is very unusual, and more "open" than in other Pt–Ru mixed-metal clusters containing Pt_3 triangular motifs: the Pt_3 unit here extends away from the Ru_6 octahedron, the third Pt atom being free from any bond to the Ru core. The plane defined by the three platinum atoms is almost perpendicular to the Ru(1)–Ru(2) bond (see side view shown in Fig. 14). It must be said that platinum has a natural tendency to form triangular motifs, but it is quite unusual to obtain such a clear segregation between the two metals. Metal segregation is usually observed for gold- or mercury-containing clusters, due to the propensity of those

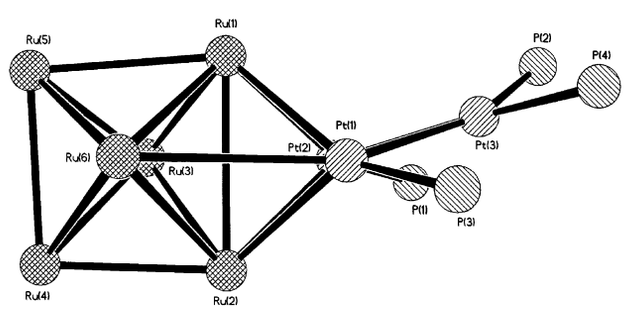

Fig. 14 Side view of the metallic core in $[Ru_6C(CO)_{16}Pt_3(dppm)_2]$ **21**.

elements to self-agglomerate (phenomenon termed "aurophilicity" in the case of gold).[25,26] The phosphorus atoms of both dppm ligands lie almost in the plane of the Pt_3 triangle, bridging the two free Pt–Pt edges. The bridging CO and dppm ligands are disposed in a very symmetrical manner on each side of a pseudo-mirror plane defined by the carbide and four Ru atoms (Ru(1), Ru(2), Ru(4) and Ru(5)). The Pt–Pt distances are in accord with the existence of such a mirror plane perpendicular to the plane of the Pt_3 triangle, and bisecting the longer Pt(1)–Pt(2) bond. The two bridging dppm ligand appear normal in every respect: the P–Pt bonds are forming angles of roughly 90° with the Pt–Pt bonds and the phosphorus and PCH_2P carbons atoms are tetrahedral. It seems reasonable to assume that these bridging diphosphine ligands are indispensable for the stability of such a structure containing an "external" Pt_3 triangle. Homometallic triangular Pt_3 com-

pounds bearing dppm ligands are very common. This tends to suggest that the $Pt_3(dppm)_2$ unit formed in solution prior to addition to the Ru_6 cluster. The geometry observed for cluster **21** (122 total electron count for the formulation $[Ru_6C(CO)_{16}Pt_3(dppm)_2]$) could have been predicted by using the fused polyhedra theory, by considering that it consists of an octahedron ($86e^-$), a triangle ($48e^-$), and two tetrahedra ($2 \times 60e^-$), with two summits ($2 \times 18e^-$) and two triangular faces ($2 \times 48e^-$) in common, giving a total of 122 electrons.

The fact that we obtained this very unusual molecular structure for $[Ru_6C(CO)_{16}Pt_3(dppm)_2]$ **21** allows us now to propose a structure for $[Ru_6C(CO)_{15}Pt_2(dppm)]$ **20**. By analogy, it seems logical that both platinum atoms are bound together, and that the Pt–Pt dimer is held together by a bridging dppm ligand, giving the structure shown in Fig. 15. However, this structure does not fit with the total electron count of 106 for cluster **20**.

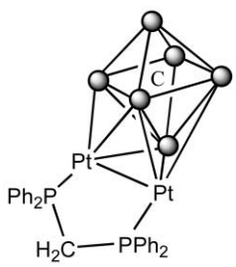

Fig. 15 Structure proposed for $[Ru_6C(CO)_{15}Pt_2(dppm)]$ **20**. Shaded circles represent Ru. Carbonyls omitted for clarity.

The mechanism by which these four clusters (**15**, **19**, **20**, and **21**) were produced from $[Ru_6C(CO)_{16}Pt(COD)]$ **2** and dppm is unclear, but two main processes seem to be important. The first one involves substitution of the Pt(COD) unit for one (and subsequently a second) dppm ligand, to form $[Ru_6C(CO)_{15}(dppm)]$ **15** and $[Ru_6C(CO)_{13}(dppm)_2]$ **19**. The second one deals with the formation *in situ* of Pt_2 dimers and Pt_3 triangles stabilised by bridging dppm ligands, which then add to a $[Ru_6C(CO)_{16}]$ unit (or replace the Pt(COD) fragment in the starting complex) and lead to $[Ru_6C(CO)_{15}Pt_2(dppm)]$ **20** and $[Ru_6C(CO)_{16}Pt_3(dppm)_2]$ **21**. These two mechanisms are probably interconnected, the first one releasing the platinum necessary for the second.

In order to gain further insight into the mechanism of formation of compounds **15** and **19**, the cluster $[Ru_6C(CO)_{17}]$ **5** was reacted directly with dppm, in dichloromethane, under refluxing conditions. Slightly surprisingly, $[Ru_6C(CO)_{15}(dppm)]$ **15** was obtained in 47.5% yield, together with two new compounds: $[Ru_6C(CO)_{14}(dppm)_2]$ **22** in 10.6% yield, and an orange product in very low yield (which remained uncharacterised). The cluster $[Ru_6C(CO)_{15}(dppm)]$ **15** was identified on the basis of its IR, mass, and NMR spectra, which fitted with data from the literature,[15] as well as the results described above. The second compound was formulated as $[Ru_6C(CO)_{14}(dppm)_2]$ **22** on the basis of elemental analysis and spectroscopic evidence. Its colour and IR spectrum did not have anything in common with the data discussed above for $[Ru_6C(CO)_{13}(dppm)_2]$ **19**. Two non-equivalent dppm ligands were detected by ^{1}H-NMR. The phenyl rings gave rise to multiplets in the range 7.57–7.10 ppm (integral: 40H), while the PCH_2P units were found as two triplets at 5.04 (integral: 2H) and 4.80 ppm (integral: 2H). Three signals were found in the ^{31}P-NMR: two doublets at 25.88 and 18.40 ppm, and a singlet at 19.39 ppm. The singlet must correspond to the two equivalent phosphorus nuclei of a bidentate dppm. The two doublets, with similar intensities, correspond to the two non-equivalent phosphorus nuclei of a monodentate dppm. The signal at 25.88 ppm can be associated with the Ru–bound end, while the signal at 18.40 ppm is assigned to the pendant end.[27] This allowed us to propose the structure shown in Fig. 16 for $[Ru_6C(CO)_{14}(dppm)_2]$ **22**. When counting

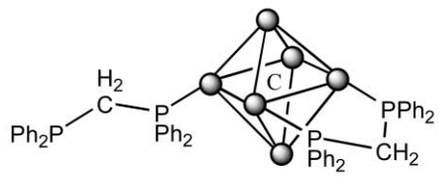

Fig. 16 Structure proposed for $[Ru_6C(CO)_{14}(dppm)_2]$ **22**. Shaded circles represent Ru. Carbonyls omitted for clarity.

the electrons in cluster **22**, the two dppm ligands were given different electron-donating capabilities: the bidentate dppm gives four electrons, while the monodentate dppm gives only two, giving a total electron count of 86 for $[Ru_6C(CO)_{14}(dppm)_2]$ **22**, corresponding to an octahedral metal core geometry. The uncharacterised orange product is speculatively suggested to be $[Ru_6C(CO)_{13}(dppm)_2]$ **19**, where both dppm are bidentate and equivalent. The isolation of $[Ru_6C(CO)_{14}(dppm)_2]$ **22** with one monodentate dppm sheds light on the mechanism of formation of dppm-cluster derivatives. It can be viewed simply as an intermediate, needing the fourth phosphorus to substitute for one more CO ligand to give $[Ru_6C(CO)_{13}(dppm)_2]$ **19**.

Conclusion

In this paper, we have described ligand substitution reactions involving the Ru–Pt clusters $[Ru_5C(CO)_{14}Pt(COD)]$ **1** and $[Ru_6C(CO)_{16}Pt(COD)]$ **2**. Only the reactions starting with $[Ru_5C(CO)_{14}Pt(COD)]$ **1** were selective. Substitution of the COD ligand by PPh_3 gave $[Ru_5C(CO)_{14}Pt(PPh_3)_2]$ **8** selectively, while with dppm the main product of the reaction was $[Ru_5C(CO)_{14}Pt(\mu\text{-dppm})]$ **10**. On the other hand, the reactions involving $[Ru_6C(CO)_{16}Pt(COD)]$ **2** led mainly to extrusion of the Pt(COD) fragment and formation of Ru-only phosphine derivatives. More precisely, with triphenylphosphine, the two clusters $[Ru_6C(CO)_{16}PPh_3]$ **16** and $[Ru_6C(CO)_{15}(PPh_3)_2]$ **18** were obtained, while with dppm, the compounds $[Ru_6C(CO)_{15}(dppm)]$ **15** and $[Ru_6C(CO)_{13}(dppm)_2]$ **19** were formed. In the latter case, two additional products of high interest were isolated (although in very small yields): $[Ru_6C(CO)_{15}Pt_2(dppm)]$ **20** and $[Ru_6C(CO)_{16}Pt_3(dppm)_2]$ **21**. The explanation for the difference in reactivity of the two Ru–Pt(COD) mixed-metal clusters might be sought in their structures. The Pt(COD) fragment capping a triangular face in $[Ru_6C(CO)_{16}Pt(COD)]$ **2** is not as strongly bound as in $[Ru_5C(CO)_{14}Pt(COD)]$ **1**, where it is part of the octahedral core. So when reacting $[Ru_6C(CO)_{16}Pt(COD)]$ **2** with phosphines, the whole Pt(COD) unit is substituted rather than the COD ligand only. The same result was obtained when reacting both clusters with carbon monoxide: the Ru_5Pt cluster gave selectively $[Ru_5CPt(CO)_{16}]$ **3**, while the Ru_6Pt cluster lost either a ruthenium or the Pt(COD) unit in the reaction. The fact that the reactions involving $[Ru_5C(CO)_{14}Pt(COD)]$ **1** were really selective means that this type of ligand exchange could be used to tether this cluster to functionalised surfaces. This aspect is under further exploration.

Experimental

All the reactions were carried out using standard Schlenk techniques, under water- and oxygen-free nitrogen. All solvents were dried and distilled immediately before use. Reactants and chemicals were purchased from Aldrich Chemicals and used without further purification. The clusters $[Ru_5C(CO)_{14}Pt(COD)]$ **1**,[3] $[Ru_6C(CO)_{16}Pt(COD)]$ **2**[3] and $[Ru_6C(CO)_{17}]$ **5**[28] were synthesised following published procedures.

All chromatographic separations were performed on the open bench without any precaution to exclude air. Thin-layer chromatography (TLC) was carried out using glass plates (20 × 20 cm) coated with a layer of silica gel 60 F254, supplied by

Merck. The eluents used were standard grade laboratory solvents.

Infrared spectra were collected in dichloromethane solution unless otherwise stated, using a NaCl liquid cell (0.5 mm path length) supplied by Specac Ltd., on a Perkin-Elmer Paragon 1000 FT-IR spectrometer. The mass spectra were obtained on a Kratos Concept spectrometer (*) and on a Kratos MS890 spectrometer (†), using electron impact ionisation (EI) in positive mode or on a Micromass Quattro-LC spectrometer using electrospray ionisation technique (ESI) in negative mode (‡). The ^{13}C- and ^{1}H-NMR spectra were recorded on a Bruker AM-400 or DPX-400 instrument, while ^{31}P-NMR spectra were recorded on Bruker AC-250 ([a]) or DPX-400 ([b]) instruments, using 5 mm quartz tubes. The elemental analyses were made by the microanalysis service of the department. It should be noted that the discrepancies observed between calculated and obtained values are due to the presence of solvent in the crystalline solids submitted for elemental analysis. This fact has been confirmed by crystallography (presence of solvent molecules in the crystal structures—see Table 5).

Reaction of $[Ru_6C(CO)_{16}Pt(COD)]$ 2 with carbon monoxide

$[Ru_6C(CO)_{16}Pt(COD)]$ **2** (60 mg) was dissolved in dichloromethane (40 ml). Carbon monoxide was bubbled through the solution, and the reaction monitored by IR and spot TLC after 5, 15, 30 minutes, 3 hours and 24 hours. The CO supply was then discontinued, and the solvent removed on a rotary evaporator. Three products, $[Ru_3(CO)_{12}]$ **4** (yellow), $[Ru_5CPt(CO)_{16}]$ **3** (red) and $[Ru_6C(CO)_{17}]$ **5** (orange), were separated by thin-layer chromatography, using hexane–dichloromethane (7 : 3, v/v) as eluent.

Analysis for $[Ru_3(CO)_{12}]$ 4. IR(CH_2Cl_2): ν_{CO}: 2060(s), 2028(s), 2009(w, sh) cm^{-1}. EI-MS(†): *m*/*z*: 640 (calc. for $Ru_3(CO)_{12}$: 639, M^+), with CO ligand losses observed.

Analysis for $[Ru_5CPt(CO)_{16}]$ 3. IR(CH_2Cl_2): ν_{CO}: 2065(s), 2050(s), 2005(w, sh), 1874(w, br) cm^{-1}. EI-MS(†): *m*/*z*: 1160 (calc. for $Ru_5CPt(CO)_{16}$: 1161, M^+), with the loss of 16 CO ligands observed. Single crystals suitable for X-ray diffraction analysis have been obtained by slow diffusion of hexane in a dichloromethane solution of $[Ru_5CPt(CO)_{16}]$ **3**. Their unit cell dimensions fitted with those obtained previously for $[Ru_5CPt(CO)_{16}]$ **3**.[4]

Analysis for $[Ru_6C(CO)_{17}]$ 5. IR(CH_2Cl_2): ν_{CO}: 2067(s), 2047(s), 2002(w, sh), 1838(w, br) cm^{-1}. EI-MS(*): *m*/*z*: 1098 (calc. for $Ru_6C(CO)_{17}$: 1095, M^+), with the loss of 17 CO ligands observed. Crystals suitable for X-ray crystallography were grown by slow diffusion of hexane into a dichloromethane solution of **5**. Their unit cell dimensions fitted with those obtained previously for $[Ru_6C(CO)_{17}]$.[18]

Reaction of $[Ru_5C(CO)_{14}Pt(COD)]$ 1 with PPh_3

$[Ru_5C(CO)_{14}Pt(COD)]$ **1** (60 mg, 0.0495 mmol) and triphenylphosphine (PPh_3, 13 mg, 0.049 mmol) were dissolved in dichloromethane (30 ml). The mixture was stirred at room temperature for 7 hours. The solvent was then removed on a rotary evaporator. The crude product was purified by thin-layer chromatography, using hexane–dichloromethane (3 : 2, v/v) as eluent, giving the orange $[Ru_5C(CO)_{14}Pt(PPh_3)_2]$ **8** in 43.6% yield (35.2 mg). IR(CH_2Cl_2): ν_{CO}: 2069(m), 2030(s), 2022(s), 1992(w), 1973(w), 1817(w, br) cm^{-1}. EI-MS(*): *m*/*z*: 1527 (calc. for $Ru_5C(CO)_{13}Pt(PPh_3)(PPh_2)$: 1528), with the loss of two Ph ligands and subsequently 13 CO ligands observed. ^{1}H NMR [CD_2Cl_2] δ: 7.73–7.40 (m, Ph) ppm. ^{13}C NMR [CD_2Cl_2] δ: 201.99 (s, CO), 200.04 (m, CO), 134.55–128.44 (CH), 134.00 (C), 133.73 (C) ppm. ^{31}P-NMR([b]) [CD_2Cl_2] δ: 41.82 (s), 29.91 (s + d) ppm. Anal. calc. for $C_{51}H_{30}O_{14}P_2Pt_1Ru_5$: C, 37.60; H, 1.86. Obtained: C, 38.50; H, 2.10%.

When the same reaction was performed with an excess of PPh_3, two compounds were isolated by thin-layer chromatography, using hexane–dichloromethane (3 : 2, v/v) as eluent: the main product, purple $[Ru_5C(CO)_{13}(PPh_3)_2]$ **9**, and a brown compound in very low yield. Analysis for $[Ru_5C(CO)_{13}(PPh_3)_2]$ **9**: IR(CH_2Cl_2): ν_{CO}: 2067(m), 2043(s), 2012(s), 1987(w, sh), 1953(m, br) cm^{-1}. EI-MS(*): *m*/*z*: 1034 (calc. for $Ru_5C(CO)_9(PPh_3)$: 1032), with the loss of CO ligands and subsequently one Ph ligand observed. ^{1}H NMR [CD_2Cl_2] δ: 7.48–7.29 (m, Ph) ppm. ^{13}C NMR [CD_2Cl_2] δ: 201.61 (C), 136.83–130.54 (CH) ppm. ^{31}P-NMR([a]) [CD_2Cl_2] δ: 37.56 ppm. Crystals suitable for X-ray diffraction structure determination were obtained by layering a dichloromethane solution of **9** with ethanol, and the formulation $[Ru_5C(CO)_{13}(PPh_3)_2]$ was confirmed.[10] Analysis for the brown compound: IR(CH_2Cl_2): ν_{CO}: 2048(m), 2013(s), 1994(m), 1991(m), 1988(m), 1956(w, sh), 1933(w, sh), 1811(w, br) cm^{-1}. EI-MS(*): *m*/*z*: 1087 (calc. for $Ru_5C(CO)_{11}(PPh_3)$: 1088), with the loss of CO ligands and subsequently one Ph ligand observed. ^{1}H NMR [CD_2Cl_2] δ: 7.55–7.23 (m, Ph) ppm. ^{31}P-NMR([b]) [CD_2Cl_2] δ: 43.39, 29.43 ppm.

Reaction of $[Ru_5C(CO)_{14}Pt(COD)]$ 1 with dppm

$[Ru_5C(CO)_{14}Pt(COD)]$ **1** (100 mg, 0.0824 mmol) and bis-(diphenylphosphino)methane (dppm, 32 mg, 0.0824 mmol) were dissolved in dichloromethane (30 ml). The mixture was stirred at room temperature for 24 hours. The solvent was then removed on a rotary evaporator. The residue was separated into its component compounds by thin-layer chromatography, using hexane–dichloromethane (3 : 2, v/v) as eluent. Three compounds were isolated: the orange $[Ru_5CPt(CO)_{16}]$ **3** (yield < 1 mg, < 1%), the main product, orange $[Ru_5C(CO)_{14}Pt(\mu\text{-dppm})]$ **10** (yield: 79 mg, 64.3%), and the orange $[Ru_5C(CO)_{11}Pt(CO)(dppm)_2]$ **11** (yield: 13.1 mg, 8.7%).

Analysis for $[Ru_5CPt(CO)_{16}]$ 3. IR(CH_2Cl_2): ν_{CO}: 2100(w), 2065(s), 2050(s), 2004(w), 1874(w, br) cm^{-1}. EI-MS(*): *m*/*z*: 1162 (calc. for $Ru_5PtC(CO)_{16}$: 1161), with the loss of 16 CO ligands observed. ^{31}P-NMR([b]) [CD_2Cl_2] δ: no signal.

Analysis for $[Ru_5C(CO)_{14}Pt(\mu\text{-dppm})]$ 10. IR(CH_2Cl_2): ν_{CO}: 2070(m), 2031(vs), 2017(m, sh), 1965(w), 1864(w, br) cm^{-1}. IR(cyclohexane): ν_{CO}: 2072(m), 2034(vs), 2018(s), 2002(m), 1987(w), 1970(w), 1876(w, br) cm^{-1}. EI-MS(*): *m*/*z*: 1494 (calc. for $Ru_5C(CO)_{14}Pt(dppm)$: 1492), with the loss of CO ligands, and consequently Ph ligands observed. ESI-MS(‡): *m*/*z*: 1520 (calc. for $Ru_5C(CO)_{14}Pt(dppm) + CH_3O$: 1520, $[M + MeO]^-$) (spectra obtained after addition of methoxide to a dichloromethane solution of the compound).[12,13] ^{1}H NMR [CD_2Cl_2] δ: 7.21–7.49 (m, 20H, Ph), 5.27 (q, 1H, J_{H-H} = 12.6 Hz, J_{H-P} = 13.2 Hz), 4.77 (q, 1H, J_{H-H} = 11.7 Hz, J_{H-P} = 12.8 Hz) ppm. ^{13}C NMR [CD_2Cl_2] δ: 199.41 (C), 137.95–137.46 (C), 133.67–128.24 (CH), 63.85 (CH_2) ppm. ^{31}P-NMR([b]) [CD_2Cl_2] δ: 22.17 (s), 20.68 (d, J_{P-P} = 37.1 Hz), −13.44 (td, J_{P-P} = 36.8 Hz, J_{Pt-P} = 3706 Hz) ppm. Anal. calc. for $C_{40}H_{22}O_{14}P_2Pt_1Ru_5$: C, 32.27; H, 1.49. Obtained: C, 32.90; H, 1.64%.

Analysis for $[Ru_5C(CO)_{11}Pt(CO)(dppm)_2]$ 11. IR(CH_2Cl_2): ν_{CO}: 2032(w), 1999(s), 1994(m, sh), 1973(m), 1950(w, sh), 1915(w), 1836(w, br) cm^{-1}. IR(cyclohexane): ν_{CO}: 2036(w), 2011(s), 2001(s), 1984(w), 1972(m), 1932(w), 1916(w) cm^{-1}. ^{1}H NMR [CD_2Cl_2] δ: 7.17–7.44 (m, 20H, Ph), 5.24 (q, 1H, obscured by solvent peak), 4.68 (q, 1H, J_{H-H} = 12.24 Hz, J_{H-P} = 12.63 Hz) ppm. ^{13}C NMR [CD_2Cl_2] δ: 221.5 (C), 133.98–128.21 (CH), 61.5 (CH_2) ppm. ^{31}P-NMR([b]) [CD_2Cl_2] δ: 16.78 (s) ppm. Anal. calc. for $C_{63}H_{44}O_{12}P_4Pt_1Ru_5$: C, 41.64; H, 2.44. Obtained: C, 41.85; H, 3.80%. Crystals of $[Ru_5C(CO)_{11}Pt(CO)(dppm)_2]$ **11** suitable for X-ray diffraction structure determination were obtained.

Table 5 Crystal data for compounds **10**, **11**, **19** and **21**

Compound	**10**	**11**	**19**	**21**
Chemical formula	$C_{40}H_{22}O_{14}P_2PtRu_5$	$C_{63}H_{44}O_{12}P_4Pt_1Ru_5$·1.5 CH_2Cl_2	$C_{64}H_{44}O_{13}P_4Ru_6$·0.5$CH_2Cl_2$	$C_{67}H_{44}O_{16}P_4Pt_3Ru_6$
M	1488.96	1944.69	1793.76	2420.59
Crystal size/mm	0.23 × 0.16 × 0.02	0.12 × 0.09 × 0.09	0.12 × 0.07 × 0.03	0.06 × 0.04 × 0.01
Crystal system	Monoclinic	Monoclinic	Monoclinic	Monoclinic
a/Å	13.3156(3)	13.3280(10)	44.576(2)	26.9740(10)
b/Å	21.2743(3)	17.7050(10)	13.3850(3)	25.6280(10)
c/Å	15.7373(4)	56.071(3)	22.5560(11)	22.1060(10)
β/°	102.7780(10)	96.710(10)	108.2280(15)	90.600(10)
U/Å^3	4347.66(16)	13140.6(14)	12782.7(9)	15280.8(11)
T/K	180(2)	180(2)	180(2)	180(2)
Space group	$P2_1/n$	$P2_1/c$	$C2/c$	$P2_1/c$
Z	4	8	8	8
μ/mm^{-1}	5.037	3.521	1.587	6.764
F(000)	2808	7512	7016	9056
λ(Mo-Kα)/Å	0.71069	0.71069	0.71070	λ(synchrotron) = 0.68910
Measured reflections	30377	41492	20791	82603
No. of indep. reflect. (R_{int})	9862 (0.0674)	22986 (0.0570)	11216 (0.0658)	29326 (0.1138)
Refinement method	Full-matrix least-squares on F^2	Full-matrix least-squares on F^2	Full-matrix least-squares on F^2	Full-matrix least-squares on F^2
Refined parameters	558	968	796	738
Final $R1$, $wR2$ [$I > 2\sigma(I)$]	0.0447, 0.1058	0.0489, 0.1103	0.0494, 0.0959	0.1166, 0.2418
$R1$, $wR2$ (all data)	0.0603, 0.1142	0.1015, 0.1786	0.0946, 0.1141	0.1540, 0.2549

Reaction of $[Ru_6C(CO)_{16}Pt(COD)]$ 2 with PPh_3

$[Ru_6C(CO)_{16}Pt(COD)]$ **2** (20 mg, 0.0148 mmol) was dissolved in dichloromethane (20 ml). Triphenylphosphine (8 mg) was added and the mixture stirred at room temperature for 3 days. The solvent was then removed on a rotary evaporator. The residue was separated into its component compounds by thin-layer chromatography, using hexane–dichloromethane (3 : 2, v/v) as eluent. Two compounds were isolated: the main product, orange $[Ru_6C(CO)_{16}PPh_3]$ **16**, and $[Ru_6C(CO)_{15}(PPh_3)_2]$ **18**.

Analysis for $[Ru_6C(CO)_{16}PPh_3]$ 16. IR(CH_2Cl_2): ν_{CO}: 2084(m), 2056(s), 2030(vs), 1983(w), 1837(w, br) cm^{-1}. EI-MS(*): *m*/*z*: 1330 (calc. for $Ru_6C(CO)_{16}(PPh_3)$: 1329), with the loss of 16 CO ligands, and consequently one Ph ligand observed.

Analysis for $[Ru_6C(CO)_{15}(PPh_3)_2]$ 18. IR(CH_2Cl_2): ν_{CO}: 2065(m), 2046(m), 2026(w, sh), 2015(vs), 1976(w, sh), 1852(w, br), 1827(w, br) cm^{-1}. EI-MS(*): *m*/*z*: 1161 (calc. for $Ru_6C(CO)_{10}(PPh_3)$: 1161), with the loss of 10 CO ligands, and consequently one Ph ligand observed.

Reaction of $[Ru_6C(CO)_{16}Pt(COD)]$ 2 with dppm

$[Ru_6C(CO)_{16}Pt(COD)]$ **2** (60 mg, 0.0438 mmol) was dissolved in dichloromethane (30 ml). Bis(diphenylphosphino)methane (dppm, 17 mg, 0.044 mmol) was added and the mixture heated under reflux. After 24 hours, the heating was discontinued, and the solvent removed on a rotary evaporator. The residue was separated into its component compounds by thin-layer chromatography, using hexane–dichloromethane (3 : 2, v/v) as eluent. Four compounds were isolated: the main product, orange $[Ru_6C(CO)_{15}(dppm)]$ **15**, the orange $[Ru_6C(CO)_{13}(dppm)_2]$ **19**, a red compound **20** in very low yield, and the brown $[Ru_6C(CO)_{16}Pt_3(dppm)_2]$ **21**. Crystals suitable for X-ray diffraction structure determination were obtained for all compounds except the red species.

Analysis for $[Ru_6C(CO)_{15}(dppm)]$ 15. IR(CH_2Cl_2): ν_{CO}: 2071(m), 2034(vs), 2017(vs), 1978(m), 1963(w, sh), 1821(m, br) cm^{-1}. ESI-MS(‡): *m*/*z*: 1390 (calc. for $Ru_6C(CO)_{14}(dppm)$: 1394). ^{1}H NMR [CD_2Cl_2] δ: 7.35 (m, 20H, Ph), 4.99 (t, 2H, J_{H-P} = 12.18 Hz, PCH_2P) ppm. ^{13}C NMR [CD_2Cl_2] δ: 204.26 (C, CO), 134.11–130.86 (CH, Ph), 89.5 (CH_2, PCH_2P) ppm. ^{31}P-NMR(a) [CD_2Cl_2] δ: 22.63 (s) ppm. Crystals of $[Ru_6C(CO)_{15}(dppm)]$ **15** suitable for X-ray diffraction analysis were obtained, and confirmed the nature of this compound, by comparison of the unit cell parameters with data from the literature.[15]

Analysis for $[Ru_6C(CO)_{13}(dppm)_2]$ 19. IR(CH_2Cl_2): ν_{CO}: 2034(m), 2004(s), 1990(m), 1977(s), 1932(w), 1794(m, br) cm^{-1}. ESI-MS(‡): *m*/*z*: 1751 (calc. for $Ru_6C(CO)_{13}(dppm)_2$: 1751), with losses of CO ligands observed.

Analysis for the red compound 20. IR(CH_2Cl_2): ν_{CO}: 2045(m), 2023(w, sh), 2014(m), 1986(s), 1972(w, sh), 1929(m) cm^{-1}. ESI-MS(‡): *m*/*z*: 1818 (calc. for $Ru_6C(CO)_{15}Pt_2(dppm)$: 1817), with losses of CO ligands and weak peaks at higher *m*/*z* observed.

Analysis for $[Ru_6C(CO)_{16}Pt_3(dppm)_2]$ 21. IR(CH_2Cl_2): ν_{CO}: 2045(m), 2024(w, sh), 2009(s), 1998(m, sh), 1982(w), 1970(m), 1945(w, sh), 1924(w, sh), 1817(m, br) cm^{-1}. ESI-MS(‡): *m*/*z*: 2420 (calc. for $Ru_6C(CO)_{16}Pt_3(dppm)_2$: 2421), with loss of CO ligands observed.

Test reaction

$[Ru_6C(CO)_{17}]$ **5** (100 mg, 0.0913 mmol) and dppm (105 mg, 0.274 mmol) were dissolved in dichloromethane (35 ml). The mixture was heated under reflux for 48 hours, after which the solvent was removed on a rotary evaporator. The residue was separated into its components by thin-layer chromatography, using hexane–acetone–dichloromethane (72.5 : 7.5 : 20, v/v) as eluent. Three compounds were isolated: the main product, orange $[Ru_6C(CO)_{15}(dppm)]$ **15** (yield: 61.9 mg, 47.5%), the purple $[Ru_6C(CO)_{14}(dppm)_2]$ **22** (17 mg, 10.6%), and an orange uncharacterised compound in low yield.

Analysis for $[Ru_6C(CO)_{15}(dppm)]$ 15. IR(CH_2Cl_2): ν_{CO}: 2071(m), 2034(s), 2017(s), 1977(w), 1962(w), 1823(w, br) cm^{-1}. EI-MS(*): *m*/*z*: 1427 (calc. for $Ru_6C(CO)_{15}(dppm)$: 1427), with the loss of CO ligands, and subsequently of three Ph ligands observed. ^{1}H NMR [CD_2Cl_2] δ: 7.28–7.41 (m, 20H, Ph), 5.01 (t, 2H, J_{H-P} = 12.18 Hz, PCH_2P) ppm. ^{13}C NMR [CD_2Cl_2] δ: 202.03 (C, CO), 135.13 (C), 134.56 (C), 131.91–128.55 (CH), 65.26 (CH_2, PCH_2P) ppm. ^{31}P-NMR(a) [CD_2Cl_2] δ: 20.77 (s) ppm. Anal. calc. for $C_{41}H_{22}O_{15}P_2Ru_6$: C, 34.61; H, 1.56. Obtained: C, 35.48; H, 1.84%.

Analysis for $[Ru_6C(CO)_{14}(dppm)_2]$ 22. IR(CH_2Cl_2): ν_{CO}: 2025(m), 2000(s), 1988(m, sh), 1968(m), 1957(w, sh), 1938(w), 1902(w, br) cm^{-1}. ^1H NMR [CD_2Cl_2] δ: 7.57–7.10 (m, 40H, Ph), 5.04 (t, 2H), 4.80 (t, 2H, J_{H-P} = 11.82 Hz) ppm. ^{31}P-NMR(^{b}) [CD_2Cl_2] δ: 25.88 (d), 19.39 (s), 18.40 (d) ppm. Anal. calc. for $C_{65}H_{44}O_{14}P_4Ru_6$: C, 43.88; H, 2.49. Obtained: C, 46.65; H, 2.96%.

Crystallography

Single crystal X-ray diffraction data for compounds **10**, **11**, and **19** were collected using a Nonius CCD diffractometer with a sealed-tube Mo-Kα source; data for **21** were collected at Daresbury SRS (UK) Station 9.8 using a Bruker AXS Smart CCD diffractometer.[29] Both instruments were equipped with an Oxford Cryosystems Cryostream cooling device. All structures were solved by direct methods using SHELXS-97,[30] and refined by full-matrix least-squares on F^2 using the SHELXL-97 software package.[30] The crystal data for these structures is summarised in Table 5. It should be pointed out that the single crystals obtained for compound **21** were extremely small, and of relatively low quality, hence the crystallographic results obtained for that compound do not meet the high standard expected. However, there was no ambiguity regarding the structure of the cluster, which is why these data are incorporated in the present manuscript, and used in the scientific discussion.

CCDC reference numbers 194575–194578.

See http://www.rsc.org/suppdata/dt/b2/b209592k/ for crystallographic data in CIF or other electronic format.

Acknowledgements

We are very grateful to John E. Davies for determining the crystal structure of compound **11**, and to Jeremy K. M. Sanders for giving us synchrotron time in Daresbury. We also wish to thank the EPSRC (for a grant to B. F. G. J., for financial assistance towards the purchase of the Nonius CCD diffractometer, and for a grant towards synchrotron time to Jeremy K. M. Sanders), the European Commission (TMR Programme) and Newnham College, Cambridge (for Research Fellowships to S. H.), and the Cambridge Overseas Trust (Schlumberger Research) and ICI (for T. K.).

References

1 R. Raja, T. Khimyak, J. M. Thomas, S. Hermans and B. F. G. Johnson, *Angew. Chem., Int. Ed.*, 2001, **40**, 4638.
2 See, for example: R. D. Adams, T. S. Barnard, J. E. Cortopassi, W. Wu and Z. Li, *Inorg. Synth.*, 1998, **32**, 280; R. Adams and W. Wu, *Organometallics*, 1993, **12**, 1248; L. J. Farrugia, *Organometallics*, 1990, **9**, 105 and references 20–24 below.
3 S. Hermans, T. Khimyak and B. F. G. Johnson, *J. Chem. Soc., Dalton Trans.*, 2001, 3295.
4 R. D. Adams and W. Wu, *J. Cluster Sci.*, 1991, **2**, 271.
5 M. I. Bruce, C. M. Jensen and N. L. Jones, *Inorg. Synth.*, 1990, **28**, 216.
6 B. F. G. Johnson, R. D. Johnston and J. Lewis, *Chem. Commun.*, 1967, 1057.
7 C. Couture and D. H. Farrar, *J. Chem. Soc., Dalton Trans.*, 1987, 2245.
8 D. H. Farrar, P. F. Jackson, B. F. G. Johnson, J. Lewis and J. N. Nicholls, *J. Chem. Soc., Chem. Commun.*, 1981, 415.
9 M. I. Bruce, G. Shaw and F. G. A. Stone, *J. Chem. Soc., Dalton Trans.*, 1972, 1781.
10 B. F. G. Johnson, J. Lewis, J. N. Nicholls, J. Puga, P. R. Raithby, M. J. Rosales, M. McPartlin and W. Clegg, *J. Chem. Soc., Dalton Trans.*, 1983, 277.
11 C. J. Adams, M. I. Bruce, B. W. Skelton and A. H. White, *J. Organomet. Chem.*, 1992, **423**, 105.
12 W. Henderson, J. S. McIndoe, B. K. Nicholson and P. J. Dyson, *J. Chem. Soc., Chem. Commun.*, 1996, 1183.
13 W. Henderson, J. S. McIndoe, B. K. Nicholson and P. J. Dyson, *J. Chem. Soc., Dalton Trans.*, 1998, 519.
14 K. Lee and J. R. Shapley, *Organometallics*, 1998, **17**, 3020.
15 T. Adatia, G. Conole, S. R. Drake, B. F. G. Johnson, M. Kessler, J. Lewis and M. McPartin, *J. Chem. Soc., Dalton Trans.*, 1997, 669.
16 S. Hermans, unpublished work.
17 S. C. Brown, J. Evans and M. Webster, *J. Chem. Soc., Dalton Trans.*, 1981, 2263.
18 A. Sirigu, M. Bianchi and E. Benedetti, *Chem. Commun.*, 1969, 596.
19 B. F. G. Johnson, S. Hermans and T. Khimyak, *Eur. J. Inorg. Chem.*, 2003, in press.
20 R. D. Adams, M. S. Alexander, I. Arafa and W. Wu, *Inorg. Chem.*, 1991, **30**, 4717.
21 R. D. Adams, Z. Li, J.-C. Lii and W. Wu, *Inorg. Chem.*, 1992, **31**, 3445.
22 R. D. Adams, Z. Li, J.-C. Lii and W. Wu, *Organometallics*, 1992, **11**, 4001.
23 R. D. Adams, Z. Li, P. Swepston, W. Wu and J. Yamamoto, *J. Am. Chem. Soc.*, 1992, **114**, 10657.
24 R. D. Adams, T. S. Barnard, Z. Li, W. Wu and J. Yamamoto, *Organometallics*, 1994, **13**, 2357.
25 D. M. P. Mingos and M. J. Watson, *Adv. Inorg. Chem.*, 1992, **39**, 327.
26 L. H. Gade, *Angew. Chem., Int. Ed. Engl.*, 1993, **32**, 24.
27 P. E. Garrou, *Chem. Rev.*, 1981, **81**, 229.
28 C. R. Eady, B. F. G. Johnson and J. Lewis, *J. Chem. Soc., Dalton Trans.*, 1975, 2606.
29 For details of a typical Daresbury data collection, see W. Clegg, M. R. J. Elsegood, S. J. Teat, C. Redshaw and V. C. Gibson, *J. Chem. Soc., Dalton Trans.*, 1998, 3037.
30 G. M. Sheldrick, SHELXS-97/SHELXL-97, University of Göttingen, Germany, 1997.
31 R. D. Adams, B. Captain, W. Fu and P. J. Pellechia, *Chem. Commun.*, 2000, 937.